

Review

Electrospun Nanofibers as Chemosensors for Detecting Environmental Pollutants: A Review

Yutong Du ^{1,*}, Deng-Guang Yu ^{1,*}  and Tao Yi ^{2,*}

¹ School of Materials and Chemistry, University of Shanghai for Science and Technology, Shanghai 200093, China

² Faculty of Health Sciences and Sports, Macao Polytechnic University, Macau 999078, China

* Correspondence: ydg017@usst.edu.cn (D.-G.Y.); yitao@mpu.edu.mo (T.Y.)

Abstract: Electrospun nanofibers have shown their advantages for applications in a wide variety of scientific fields thanks to their unique properties. Meanwhile, electrospinning is closely following the fast development of nano science and nanotechnology to move forward to smaller (pico-technology), more complicated nanostructures/nanodevices and more order (all kinds of nano arrays). Particularly, multiple-fluid electrospinning has the strong capability of creating nanostructures from a structural spinneret in a single-step and a straightforward “top-down” manner, holding great promise for creation on a large scale. This review is just to conclude the state-of-art studies on the related topics and also point out that the future directions of environmental detection require chemosensors, while the improvement of sensors requires new chemically synthesized functional substances, new nanostructured materials, application convenience, and functional integration or synergy. Based on the developments of electrospinning, more and more possibilities can be drawn out for detecting environmental pollutants with electrospun nanostructures as the strong support platform.

Keywords: pollution detection; nanostructure; chemical sensing; functional integration



Citation: Du, Y.; Yu, D.-G.; Yi, T. Electrospun Nanofibers as Chemosensors for Detecting Environmental Pollutants: A Review. *Chemosensors* **2023**, *11*, 208. <https://doi.org/10.3390/chemosensors11040208>

Academic Editors: Eduardo Torres and Ilaria Palchetti

Received: 11 February 2023

Revised: 16 March 2023

Accepted: 22 March 2023

Published: 25 March 2023



Copyright: © 2023 by the authors. Licensee MDPI, Basel, Switzerland. This article is an open access article distributed under the terms and conditions of the Creative Commons Attribution (CC BY) license (<https://creativecommons.org/licenses/by/4.0/>).

1. Introduction

At present, people are paying more attention to three environmental issues: the greenhouse effect, ozone layer destruction, and acid rain. This is because environmental pollution has begun to threaten human safety, and the harm caused by environmental pollution to human health is very complex. Taking carcinogenesis as an example, the World Health Organization believes that a large part of human cancer is caused by chemicals found in environmental pollution. Environmental pollution is mainly manifested in the air, water, and soil [1–3]. Clean air is mainly composed of nitrogen, oxygen, argon, and a small amount of carbon dioxide and water vapor, as well as trace amounts of rare gases. However, when the atmospheric composition changes and reaches a crisis level for organisms, it causes air pollution. The sources of air pollution are both natural and manmade. Natural pollution sources include soot, sulfur oxides, and nitrogen oxides produced by earthquakes and volcanic eruptions [4–8]. Manmade sources of pollution arise from human activities, especially in industry and transportation. At present, air pollutants mainly include dust, heavy metals, sulfur oxides, nitrogen oxides, carbide, and so on. There are a variety of toxic substances on the surface of dust particles, which can cause respiratory tract, heart, and lung diseases after entering the human body [9–12]. Sulfur dioxide released into the atmosphere often combines with water vapor to form sulfuric acid smoke, which is highly corrosive, while nitrogen oxides can produce a toxic photochemical smog. Carbon monoxide is an odorless and highly cumulative toxic gas that can be maintained in the atmosphere for two or three years [13–17]. Water is a precious resource for mankind, without which there is no life. However, water pollution is quite serious in the world; the main sources of water pollution are hospital sewage and untreated industrial and domestic wastewater. Water pollution occurs when the harmful substances

in the water exceed the self-purification capacity. These harmful substances include heavy metals and their compounds, organic and inorganic chemicals, pathogenic microorganisms, and radioactive substances [18–21]. Pathogenic microorganisms in sewage can cause the spread of infectious diseases; metal compounds can cause chronic poisoning of the human body; and organic poisons such as benzene, dichloroethane, and ethylene glycol can poison aquatic organisms and affect aquatic life [22–24]. Water pollution is not only a serious threat to animal and plant health, but it is also harmful to land and air. Organic matter in sewage undergoes anaerobic decomposition, producing hydrogen sulfide, thiol, and other deleterious gases, which pollute the air. Groundwater and surface water are also polluted through infiltration [25–27]. Land pollution occurs when soil accepts certain pollution due to its own characteristics and has a limited self-purification capacity. Chemical substances can invade the soil, causing the original physical and chemical properties of soil to deteriorate, thus decreasing the land's production potential [28–30]. The main pollutants polluting the soil include inorganic pollutants (heavy metals), organic pesticides, organic wastes (refractory organic waste), sludge, fly ash, and radioactive substances [31–33]. Land pollution will directly lead to the deterioration of soil properties in terms of eco-environmental effects, resulting in the reduction of vegetation and biodiversity. In addition, land pollution may also cause secondary environmental problems such as threatening ecological security and air and water pollution [31,34]. In addressing the issue of environmental pollution, comprehensive integrated control can be achieved by combining pollution abatement and environmental monitoring [35,36].

Detecting environmental pollution has always been a concern. It involves detecting the content of inorganic and organic pollutants in the environment to maintain environmental quality and safety. Several complex analytical instruments can be used to accurately detect the quantitative information of metal ions in the environment, including inductively coupled plasma–mass spectrometry (ICP-MS), surface-enhanced Raman spectroscopy (SERS), X-ray fluorescence spectroscopy (XPS), and atomic absorption spectroscopy (AAS) [37,38]. However, these methods are expensive, complicated, and time-consuming, making them unsuitable for field measurement. Therefore, researchers have been developing field-detection sensor devices that provide a short response time, high sensitivity, and selectivity. A sensor is an analytical equipment used to identify analytes, consisting of receptors, physical and chemical signal sensors, and processors. The working principle of the sensor can be divided into magnetic, mechanical, electrochemical, and optical principles according to the type of output signal [39–44]. Electrochemical and optical chemical sensors have received great attention in sensing detection, as they can perform real-time detection without the use of complex spectroscopic instruments. Electrochemical techniques have been widely used due to their high sensing performance, low detection limit, simplicity, and ability to detect different substances simultaneously [45–47]. Its good sensitivity and selectivity, low cost, lightness and portability, field-detection suitability, simple operation, and short time response can be divided into fluorescence and colorimetric sensing according to their mechanism [48–50]. Moreover, the successful development of these detection sensors using electron transfer and energy transfer mechanisms is related to the nature of the constructed platform [51]. With the development of nanomaterials, sensor platforms that realize the transduction technology are emerging, such as graphene, quantum dots (QDs), nanotubes, molecular imprinted polymer (MIP), metal–organic framework (MOF), and nanoparticles (NPs). These materials can significantly improve the sensors in terms of sensitivity, selectivity, response time, multi-channel detection capabilities, and portability. Researchers have also successfully designed sensors that depend on different light signal transduction systems [40,45,52–56]. Nanofibers (NFs) can be applied not only to electrochemical sensors but also to optical sensors. NFs can be produced by a variety of methods, such as the melting method, wet spinning, self-catalyst growth, sacrificial template method, vapor deposition method, thermal evaporation method, and electrospinning. However, NFs prepared by electrospinning have the advantages of easy man-

ufacturing and functionalization, low cost, convenient detection, multiple structure, and high porosity [11,27,57–59].

Electrospinning technology can create unique structures and various functional properties in NFs. By combining polymer, metal, metal oxide, and active ingredients, using electrospinning technology and postprocessing mixed nanocomposite materials or Janus, core-shell, hollow, and porous structures with unique functional NFs can be prepared. Electrospun NFs have superior mechanical properties and excellent surface characteristics, making them ideal for use in energy, environmental, medical, and food-related applications [60,61]. Therefore, the sensor platform made from electrospun NFs is characterized by easy preparation and function, low cost, flexibility, and mechanical stability. Moreover, the electrospun NF sensor platform is portable, making it suitable for field detection. Various functionalization means, including direct blending and postprocessing, can be used to achieve high selectivity and multiplex detection capability. Since the application of electrospinning in sample preparation, many papers have been published in the sensing field, and the number of publications on electrospun NF-based sensors has increased rapidly. The numbers of publications of sensors and electrospun NF-based sensors between 2012 and 2022 are shown in Figure 1. This paper describes the research progress and the advantages of electrospinning technology in preparing different structured NFs for the detection nanomaterials.

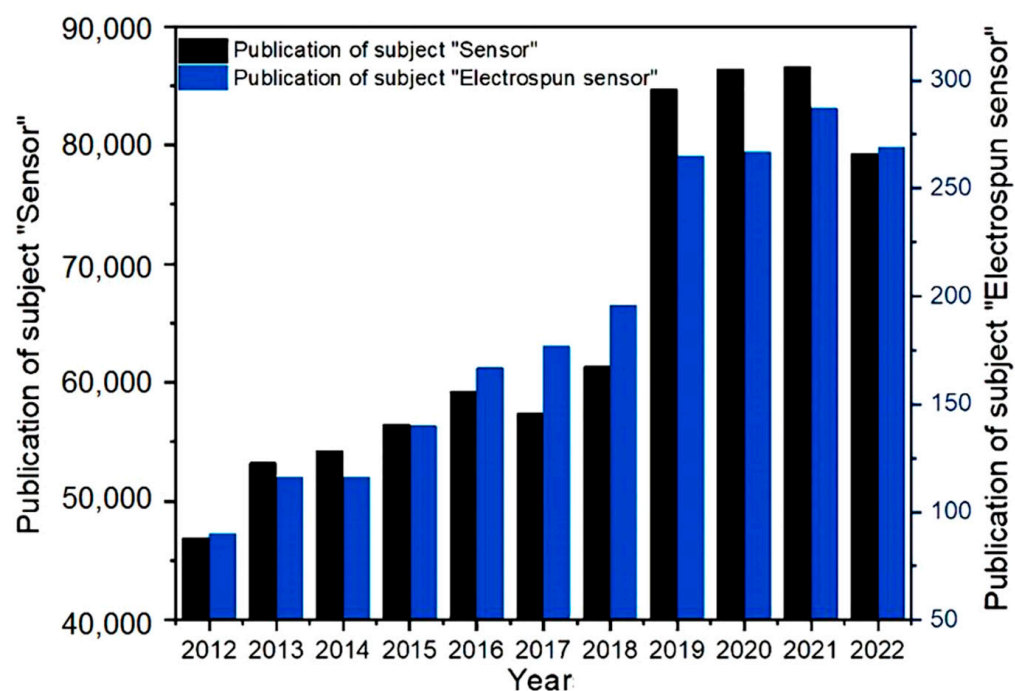


Figure 1. The literature search statistics using the themes “Sensor” and “electrospinning and electric spinning sensor” on the Web of Science platform.

2. Electrospinning

Nanomaterials, due to their special structure and a series of unique physical and chemical properties, are widely used in chemosensors, e.g., for the fixation of active molecules, signal detection, and transmission amplification; greatly improve the sensitivity; shorten the response time; and achieve high-throughput real-time detection, providing a new research path and huge space for the development of chemosensors [62–69]. NFs have become a hot spot in sensing research due to their unique structure, and the electrospinning process can directly and continuously prepare polymer NFs [70–73]. The experimental setup for electrospinning technology consists of three parts: a high-voltage power supply, a spinning device, and a collection plate (Figure 2A). The positive termi-

nal of the power supply output by the power supply is connected to the needle of the syringe, and the negative terminal is connected to the receiving plate [74–76]. When the electric field force and surface tension of the spinning liquid are equal, a “Taylor cone” will be formed at the spinneret, and the electric field force can overcome the surface tension of the liquid by further increasing the voltage, and the charged liquid will be ejected from the spinnerets in the form of fiber bundles and received by the receiver [76–80]. After a series of bending and stretching processes, the diameter is continuously reduced, while the solvent gradually volatilizes, and then the dried NFs fall on the receiving plate [81–84]. Polymer chains can be rapidly frozen during electrospinning, effectively inhibiting intermolecular π – π interactions [85]. Electrospun NFs have the advantages of a small structure size and large specific surface area, which have a good role in improving the sensitivity, response time, and selectivity of sensors, so they have great potential in the sensor field. In recent years, electrospinning technology has developed from single-fluid to multi-fluid electrospinning technology; due to the high requirements of the single-fluid electrospinning process on the spinnability of materials, only the simplest single-layer NFs can be prepared in practical applications, thus creating great limitations. Multi-fluid electrospinning technology can prepare complexly structured and functional NFs, which can be divided into coaxial, side-by-side, and multistage electrospinning technology. The prepared NFs will have a core–shell structure, Janus structure, or tertiary core–shell/Janus structure (Figure 2B).

Conventional coaxial electrospinning techniques have limitations, such as the requirement for the sheath fluid to be spinnable, high solution concentration, and blockage of the spinneret during the implementation process. These factors can lead to poor control of the fiber morphology and diameter [86–88]. To address these challenges, researchers have developed modified coaxial electrospinning methods, which regulate the release of active substances, using specialized structures [89]. The improved coaxial electrospinning method uses non-spinnable liquids, such as pure solvents, dilute polymer solutions, or emulsions, as the sheath working fluid to prepare fibers. This method improves the quality of NFs and allows for the adjustment of the fiber size. Core–shell NFs can be prepared using coaxial spinnerets, while Janus fibers can be prepared using parallel capillary spinnerets. Spinnerets consisting of parallel capillaries provide structural templates for producing Janus fibers. Janus fibers have two sides in direct contact with the surrounding environment and exhibit unique properties compared to core–shell fibers [90–92]. Li et al. prepared drug-loaded Janus beads-on-a-string-structure NFs by using a parallel spinneret with a sleeve made of polytetrafluoroethylene (PTFE), demonstrating bipolar controlled release [91]. However, parallel spinnerets fail to prepare NFs with a parallel structure due to the ease of separation of the double fluids with small contact area [93–96]. To address this limitation, researchers designed eccentric parallel spinnerets. The rounded outer metal capillaries made the charge evenly distributed on the surface, and sufficient contact area between the two working fluids was provided to prevent separation [97–99]. The Janus structure produced by the electrospinning process can be tailored by adjusting the spinning parameters to customize the properties of the two-layer Janus nanofibers, such as the ratio of each component, the distribution of active components, and the properties of the polymer matrix. It can be effectively used for the development of new nanomaterials [100–102].

Multifluid electrospinning technology is also increasingly used in various fields. Yang et al. demonstrated a preparation of functional three-layer NFs by using tertiary coaxial electrospinning [101]. The NFs utilized cellulose acetate (CA) and polyvinylpyrrolidone (PVP) as drug carriers, and the middle blank CA layer enabled precise two-stage drug release. While the development of tertiary structures is still in its early stages, research is exploring the combination of coaxial and Janus structures to form three-level structures with diversified parallel coaxial and coaxial parallel arrangements [103–108]. Generally, hollow NFs need to be obtained under an inert atmosphere or after freeze-drying [109–111]. However, the development of coaxial electrospinning technology has enabled the one-step preparation of hollow NFs. The principle of preparing hollow NFs is similar to that of solid

NFs, but the spinning parameters and post-treatment need to be adjusted. Irfan et al. used a coaxial double capillary filament head with PVP as the sheath fluid and a salt solution as the core fluid to prepare hollow NFs through selective calcination [112]. By controlling the experimental parameters, the inner diameter and wall thickness of these hollow NFs can range from tens of nanometers to hundreds of nanometers, and the core and sheath fluids can be modified independently to achieve NF functionalization [111,113–115]. Liu et al. made hollow NFs composed of copper oxide (CuO) and polyaniline (PANI) [111]. The electrospinning technique was employed to fabricate hybrid NFs, which demonstrated outstanding electrochemical characteristics in detecting hydrogen peroxide (H₂O₂) and glucose without the need for enzymes. The hollow NFs possess several noteworthy attributes, including their considerable surface area, high porosity, and distinctive structure, rendering them a suitable choice for sensing materials. Notably, the hollow configuration of the NFs facilitates the diffusion of analyte molecules into the nanofiber, thereby enhancing the sensitivity and selectivity of H₂O₂ and glucose detection (Figure 2C). The resulting hollow structure of these fibers increases their surface area and capacitance. Conductive nanoparticles are added to enhance their electrochemical performance through reversible redox reactions. The supercapacitors fabricated using these fibers show excellent properties, making them potential candidates for future energy storage systems. Yin et al. prepared cobalt–iron selenides (CoFe₂Se₄) porous carbon NFs (PCF), using Prussian blue analogues, as a novel phenolic chemosensor for detecting gases [113]. The nanocomposites produced through the use of three-dimensional (3D) network nanostructures offer an optimal conductive network that promotes electron transfer and inhibits the aggregation of nanoparticles. By utilizing porous NF-modified electrodes, hydroquinone (HQ), catechol (CC), and resorcinol (RS) were simultaneously detected with excellent electrochemical performance and multiplexing ability. The porous structure and high conductivity of the NFs make them an ideal support material for chemosensors, resulting in a synergistic effect that enhances electrocatalytic performance (Figure 2D). The porous NF-based sensors obtained have a good anti-interference performance and excellent stability. When the structure of NFs is changed from solid to porous, the fiber specific surface area can be increased, and increasing the surface area is conducive to the application of NFs to the fields of catalysis, filtration, adsorption, tissue engineering, and other fields [116–121]. There are three ways to achieve porous structures in electrospun NFs, breath figures (BFs), based on selective removal of components (SR) from NFs made from composites or blended materials and the use of phase-separation methods [120]. Poudel et al. prepared three-dimensional hollow and porous carbon NFs (3DHPCNF) by coaxial electrospinning and freeze-drying and then prepared ZMA-LDH@Fe₂O₃/3DPHCNF (ZMA-LDH, ternary zinc–magnesium–aluminum layered double hydroxide) by hydrothermal synthesis double hydroxide and α -Fe₂O₃, hematite) [114].

Coaxial electrospinning is a useful technique for fabricating core–shell NFs with controlled composition and morphology. In the study, it allowed the authors to confine the ZMA-LDH and α -Fe₂O₃ nanorods within the core of the NFs, while the PVP shell prevented the nanorods from agglomerating during electrospinning. In conclusion, the use of coaxial electrospinning allowed for the fabrication of a well-defined electrode material with enhanced electrochemical properties, highlighting the potential of this technique for the development of high-performance energy storage devices. Hollow and porous interconnects increase the high surface area, and superior-conductivity layered composite electrodes provide high areal capacitance. Wang et al. doped 1,4-Dihydroxyanthraquinone (1,4-DHAQ) with cellulose (CL) by using electrospinning technology, and then 1,4-DHAQ@CL porous NFs were prepared by deacetylation for the fluorescence detection of Cu²⁺ in contaminated water [122]. Cu²⁺ was added to 1,4-DHAQ@CL to generate (1,4-DHAQ)-Cu²⁺@CL porous NF membrane to further fabricate a fluorescence sensor for detecting Cr³⁺ in aqueous solution. Fluorescence sensors are interactions between the sensing device that is modified by fluorophore and the target molecule on the sample surface, so their sensitivity with the surface area per unit mass (S/M ratio) of the modified sensor's surface. The electrospun

1,4-DHAQ @CL NF membrane is converted into a 1,4-DHAQ @CL porous NF film after deacetylation, and a higher S/M ratio can be obtained by increasing the microporous amount, which improves the sensing performance of the fluorescent sensor.

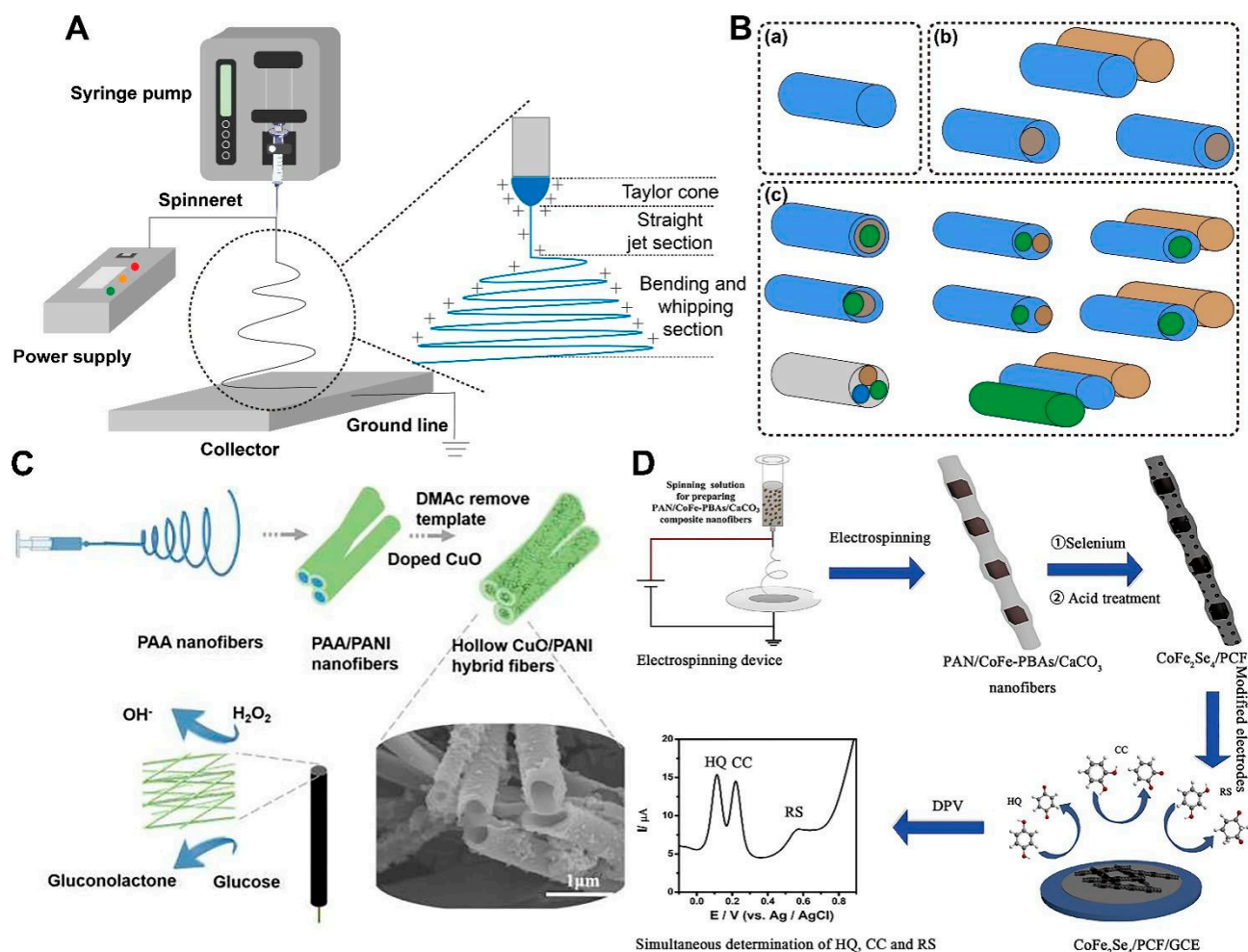


Figure 2. Schematic diagram of electrospinning process. (A) Electrospinning equipment. (B) Different processes of electrospinning. (a) Single-fluid electrospinning. (b) Two-fluid electrospinning. (c) Three-fluid electrospinning. (C) Schematic procedure of hollow CuO/PANI NFs for detection (reproduced with permission from [111], copyright © 2019, Elsevier). (D) The preparation of $CoFe_2Se_4$ porous carbon NFs (reproduced with permission from [113], copyright © 2020, Elsevier).

These structures not only increase the specific surface area of the fiber but also enhance the functionalization of the fiber, which is conducive to enhancing the sensitivity and detection range of the sensor platform. Below, we analyze the advantages of different structured nanofiber-based environmental detection sensors in environmental application areas (water, air, and soil) separately. Core-shell-structure NFs can achieve a multistage redox reaction or have multiple detection capabilities. Janus-structure NFs have biphasic controlled-release properties, thus giving them great advantages in electrochemical detection. Hollow-structure NFs greatly increase the specific surface area of fibers and can shorten the response time during sensing, and porous-structure NFs can improve the charge-transfer ability and achieve good catalytic activity, thus greatly improving the sensing performance.

3. Type of Detection Method for the Electrospun-Nanofibers-Based Chemosensors

With the development of nanotechnology, nanomaterials such as MIPs, QDs, NPs, MOFs, graphene, nanotubes, and NFs are increasingly being used as sensor platforms in various sample detection fields, including biomedical, food safety, and environmental pollution [123–129]. As a chemical-sensing platform, NFs use electrochemical and optical detection methods to greatly accelerate the sensing response time and field detection efficiency, with increasing detection range and sensitivity [130–133]. Therefore, NFs have high application prospects in chemosensors for high-precision qualitative and quantitative detection of environmental pollution. The sensor detection performance usually includes sensitivity, selectivity, detection limit (LOD), repeatability, response, and recovery time, among which good sensitivity and linear response are the keys to preparing sensors. The development of nanomaterials can effectively improve the sensor detection performance [134–139].

3.1. Electrochemical Sensor

In chemosensors, the principle can be divided into electrochemical and optical sensors. The detection principle of electrochemical sensor is based on the measured substance in the process of electrochemical sensor surface reaction, using the recognition element induction in electrochemical sensor surface and substrate combined to produce a certain biological or chemical quantity; then, through the signal converter, according to a certain rule, a quantitative electrical signal (such as current, potential difference, or conductance properties) can be programmed so as to achieve the purpose of analysis and monitoring. The change and the concentration of the substance to be analyzed are proportional to the quantitative analysis of the analyte [123,140–144]. Compared with traditional methods, the electrochemical sensor has many advantages, such as high sensitivity, a short response time, simple operation, the ability to monitor online in complex systems, and the ability to remove other analytes without the need for pretreatment, making it a unique analytical method for environmental pollution detection [145,146]. Electrochemical sensors usually use the following methods to detect environmental pollutants, namely voltammetry, amperometry, and the impedance method [143,147]. In the voltammetry method, the test substance is easily directly oxidized or reduced on the working electrode to obtain a specific oxidation-reduction potential for qualitative analysis with good selectivity [148]. The amperometry method can quantitatively analyze the concentration of the test substance by generating a specified potential through the electrolytic current [149]. The change in impedance caused by different concentrations of the test substance on the electrode surface can show a micro linear range with a low detection limit [140]. Zhang et al. prepared flexible hydrogen sulfide (H₂S) sensors, using electrospun NFs coated with a porous MOF that can detect ultralow concentrations of the gas [52]. Specifically, the researchers utilized electrospun polyvinylidene fluoride (PVDF) NFs as a substrate to grow NO₂-UiO-66, a type of MOF, resulting in a sensitive and selective H₂S sensor. Electrospinning provides a large surface area for the growth of the MOF and improves the sensitivity of the sensor. The article highlights the significance of electrospinning in sensor manufacturing and proposes that this innovative technique could pave the way for the creation of flexible gas sensors with environmental applications (Figure 3A). Song et al. prepared a sensor made of a carbon nanofiber modified with an MOF made of iron (Fe) [41]. The resulting NFs had a high surface area-to-volume ratio, and the Fe-based MOF was used to modify the surface of the carbon NFs, which enhanced the selectivity and sensitivity of the sensor. The article provides a detailed analysis of the material mechanism of electrospun NFs and the electrochemical behavior of the sensor, which can be useful for designing and fabricating other electrochemical sensors (Figure 3B).

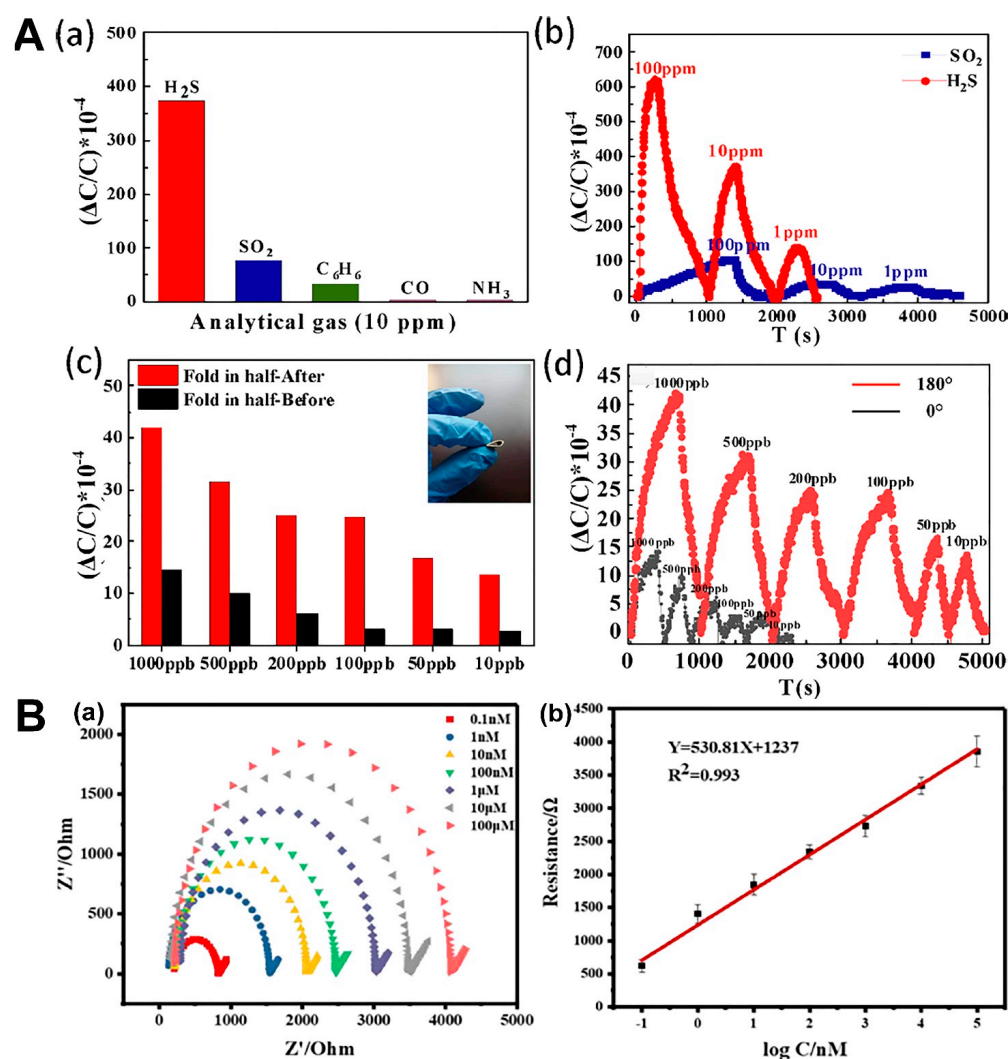


Figure 3. Application of electrochemical detection sensors in environmental pollution. (A) (a) Evaluation of the selectivity of the $\text{NO}_2\text{-UiO-66}$ nanomaterial sensor toward H_2S . (b) Detection of varying concentrations of H_2S and SO_2 , using the $\text{NO}_2\text{-UiO-66}$ nanomaterial sensor. (c) Analysis of the capacitive variations exhibited by the sensor under normal conditions and when subjected to 180° bending. (d) Investigation of the cyclic stability of the sensor for different concentrations of H_2S while subjected to bending (reproduced with permission from [52], copyright © 2022, Elsevier). (B) (a) Investigation of the impedance responses of the aptasensor toward various concentrations of TC, using EIS. (b) Generation of a calibration curve for the quantitative detection of TC, using the aptasensor (reproduced with permission from [41], copyright © 2022, Elsevier).

3.2. Optical Sensor

In the case of chemosensors, according to the principle, they can be divided into the fluorescence method and colorimetric method. The chemosensors based on the fluorescence method have the characteristics of a short response time, selectivity, and a wide detection range. Its basic principle is the specific interaction between the biomolecules on the sensor and the object to be analyzed [4,150–156]. The light signal formed by absorption or emission band changes resulting from chemical interactions is easily detected by fluorescent molecules, with the light signal correlated with the concentration of the analyte [157–165]. Nanomaterials are widely used as probe indicators in various chemical tests due to their high sensitivity, wide detection range, and convenient operation. Han et al. prepared a novel fluorescent hydrogel for the efficient adsorption and detection of hexavalent chromium (Cr(VI)) [159]. The hydrogel was created by blending lignin, cellulose

nanofibers (NFs), and carbon dots and subjecting them to electrospinning to confer fluorescence properties for detection purposes. The hydrogel exhibited a high adsorption capacity for Cr(VI) and demonstrated high sensitivity in detecting its presence through fluorescence spectroscopy. The electrospinning technology played a crucial role in developing this innovative hydrogel due to the resulting high surface area and porosity of the material (Figure 4A). Colorimetric detection is widely accepted as a selective and highly sensitive method for detecting various analytes, making it suitable for the rapid and simple detection of environmental pollution. Due to its simplicity, ease of operation, and fast field detection, colorimetric technology is currently moving toward miniaturization without additional cost. The development of chromogenic materials and their colorimetric sensing mechanism is a key research direction in the development of nanomaterials, which have played a crucial role in optical sensing equipment [159–164]. Chromogenic materials include organic materials (based on chelation reaction, self-catalyzed reaction, and enzyme-mimetic reaction), inorganic materials (based on local surface plasmon resonance, QDs, and MOFs), and other materials (such as photonic crystals) [165–169]. Hu et al. modified fibrous acid NFs that were prepared by electrospinning technology, using 2-(5-Bromo-2-pyridylazo)-5-(diethylamino) phenol (Br-PADAP) as a color developer for the quantitative detection of uranyl (UO_2^{2+}) by visual colorimetric sensing [170]. Cellulose acetate (CA) NFs were used as a matrix for immobilizing Br-PADAP, making the sensor highly portable and stable. The BR-PAPAP embedded in the fiber can interact strongly with UO_2^{2+} , which perturbs the BR-PAPAP backbone and causes color changes (Figure 4B). With the advancement of technology, smartphone-assisted colorimetric readers, which combine readout devices with colorimetric methods, have a wide range of applications in sensor applications [43,44]. In the following sections, we mainly focus on the principle of electrochemical sensing and optical sensing and discuss the research on electrospinning technology in the field of chemical sensing for environmental detection, as well as the advantages of different structured NFs in improving sensing performance.

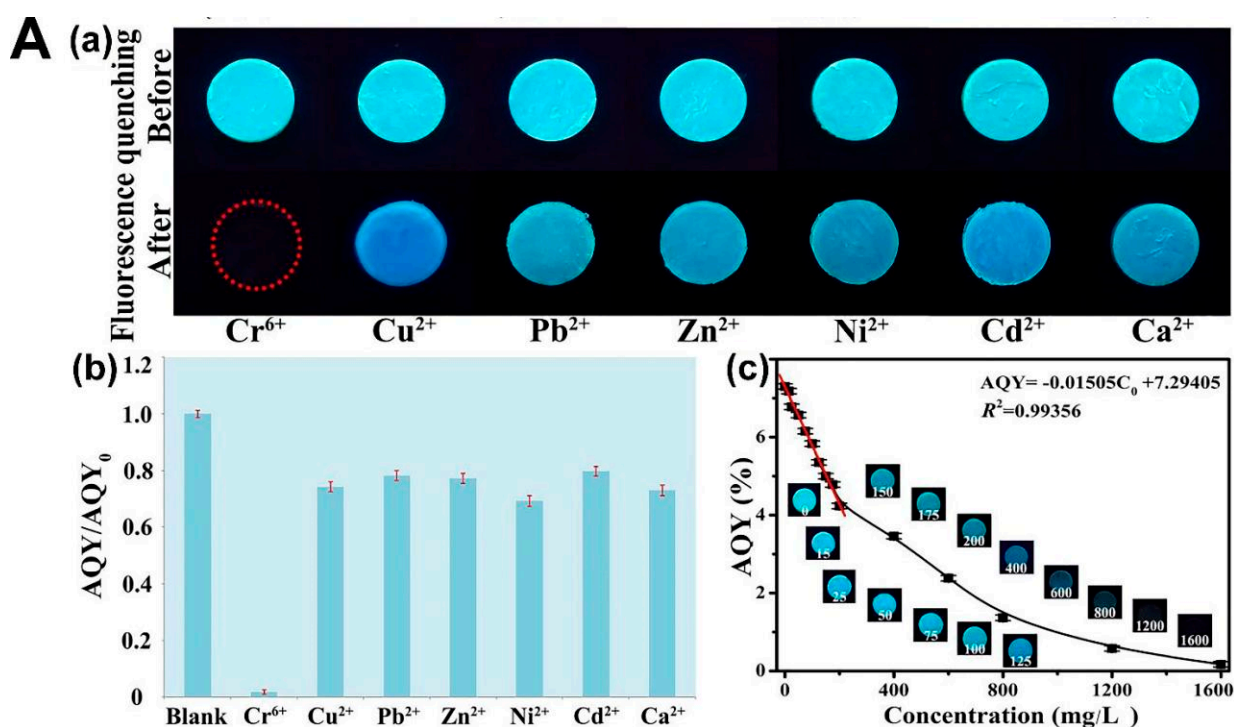


Figure 4. Cont.

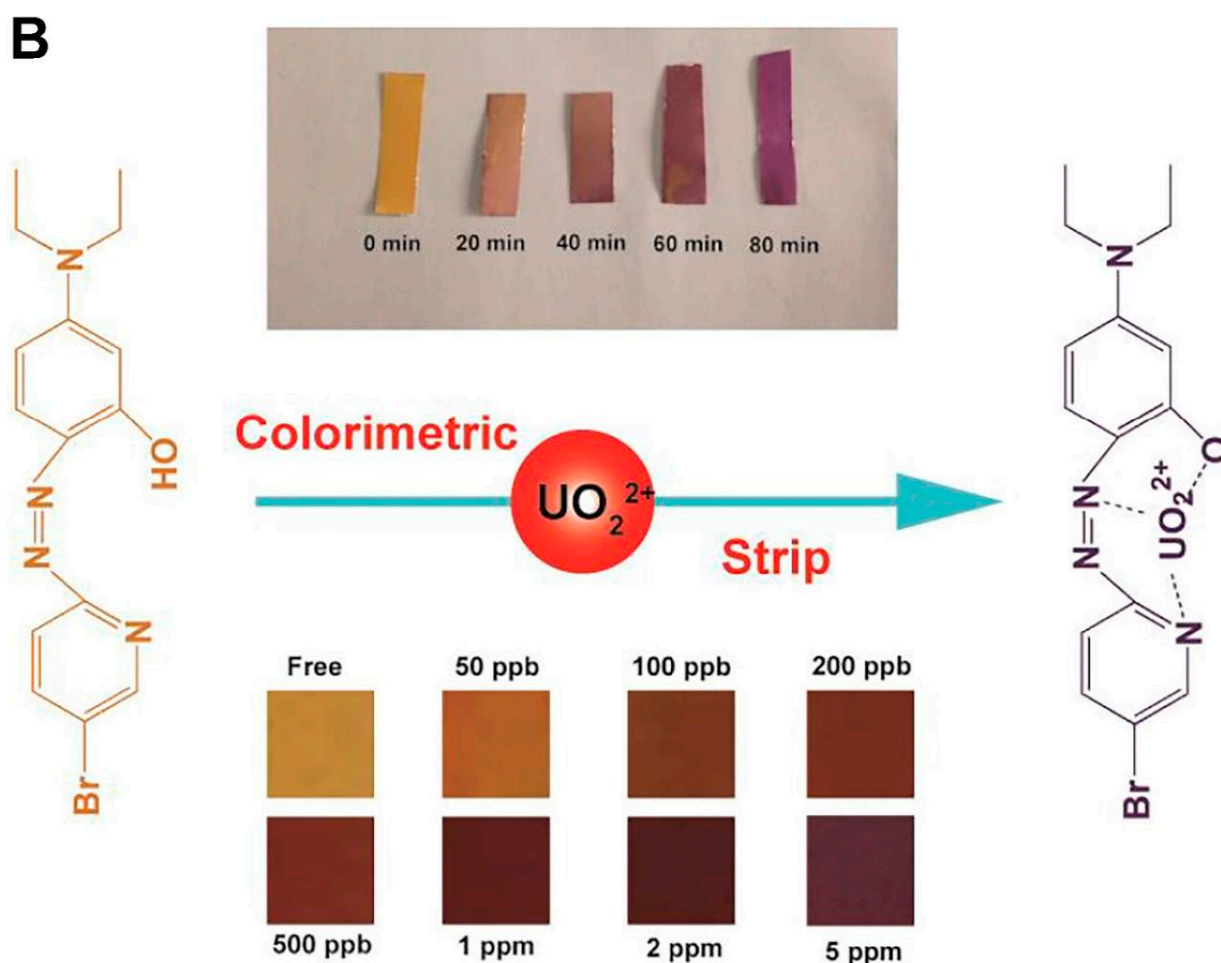


Figure 4. Application of optical detection sensors in environmental pollution. (A) (a) After adding different metal ions at a concentration of 2000 mg/L, the lignin-based hydrogel exhibited changes in its fluorescent properties. (b) The addition of various heavy metals caused the AQY (absolute quantum yield) of FLH-3, a hydrogel made from lignin, to vary. (c) The concentration of Cr(VI) had a gradual effect on the fluorescence of FLH-3, resulting in a decrease over time (reproduced with permission from [159], copyright © 2021, Elsevier). (B) The process of complex formation with uranyl ions, the duration required for colorimetric detection in photographs, and the optical colorimetric response of Br-PADAP/CA NFs at varying concentrations of UO_2^{2+} (reproduced with permission from [170], copyright © 2017, Elsevier).

4. Application Area for the Electrospun-Nanofibers-Based Chemosensors

With the acceleration of the industrialization process, pollution control has become a hot issue worldwide. Electrospinning technology has been widely applied in pollution treatment due to its own properties, including the adsorption of heavy-metal substances in water [171], filtering of the pollutants in the air [57], and catalytic degradation of organic pollutants [172]. At the same time, chemosensors prepared by electrospinning technology play an important role in environmental pollution detection. This paper introduces the application of electrospinning technology in chemosensors and explores the advantages and future prospects of different structural NFs in the development of environmental-monitoring chemosensors. Electrospun NFs often have some remarkable properties, including a special three-dimensional morphology, a large specific surface area, and ease of preparation. Excellent biocompatibility, degradability, and the ability to repeat NFs make environmental monitoring more environmentally friendly and convenient, greatly reducing the pollu-

tion in the detection process. The following presents chemosensors of NF platforms for monitoring water, air, and land pollution.

4.1. Water Pollutant

At present, due to the rapid increase of pollution sources caused by excessive industry, a large number of harmful pollutants flow into surface water and groundwater, and the concentration levels of various pollutants are increasing; particularly, dyes, drugs, pesticides, and other industrial products make water pollution a key problem in the world. Water pollutants are harmful and can have detrimental effects on both human health and the environment. They can be absorbed by plants, and through the food chain, they can cause indirect land pollution. Certain pollutants have been linked to cancer and mutagenesis, posing a significant risk to human beings. To address this problem, electrospinning technology has been utilized to prepare NFs with adjustable properties, such as a specific surface area, composition, porosity, thickness, and diameter. These NFs have been used to develop chemosensors with excellent sensing properties, allowing for the detection and analysis of water pollutants. Due to their large specific surface area and large active site, the various functional metal-modified NFs have high chemical and electrochemical stability, which helps to improve the high stability and significant conductivity of the sensor. NF-based sensors have the advantages of specificity, stability, and low cost. NFs with specific structures can be used to directly capture specific targets, bind to nanomaterials, amplify response signals, and also serve as oxygen functional groups at binding and analyte recognition sites to improve detection performance. Hua et al. demonstrated the preparation of a sulfonylcalix[4]arene-functionalized NF membrane (sulfonylcalix–NFM) as a sensor and adsorbent for the detection, identification, and enrichment of Tb^{3+} ions through electrostatic attraction loading of anion sulfonyl-calix[4]arene onto the surface of cationic NFs [173]. The adsorption mechanism of Tb^{3+} ions was attributed to the complex formation between sulfonylcalix[4]arene loaded on NFM and Tb^{3+} ions. The combination of Tb^{3+} on sulfonylcalix–NFM and sulfonylcalix[4]arene exhibited a good photoluminescent performance and selective fluorescence recognition, with a low detection limit for Tb^{3+} ions under ultraviolet radiation. The adsorption of Tb^{3+} ions onto sulfonylcalix–NFM is believed to occur via electrostatic interactions between SO_3 groups and Tb^{3+} ions, as well as through synergistic coordination of sulfonyl O and two adjacent phenoxy O^- (Figure 5). NF membranes were prepared by using electrospinning technology to achieve fluorescence recognition and enrichment adsorption of heavy metal ions, demonstrating a novel method for the development of electrospinning technology in the field of environmental detection. Chen et al. prepared porous NFs by using ultra-efficient liquid chromatography and mass spectrometry to analyze and detect residual sulfonamide in ambient water samples [174]. They found that polystyrene (PS) porous NFs were effective materials for preparing different polar sulfonamides in wastewater due to their high specific surface area, and the interaction of the formation mechanism causes phase separation of solvent and non-solvent evaporation. The surface morphology of the NFs may improve the absorption efficiency of the drugs. These results suggest that porous electrospinning NFs can be a promising adsorbent with great potential in detecting drug residues in a complex wastewater matrix. The porous structure of the NFs facilitates and accelerates the interaction between the analyte and recognition site. Qi et al. prepared core-and-shell-structure polypyrrole (PPy)-functionalized NFs that could detect trace amounts of sulfated azo dye in water in the environment [175]. The PA6/PPy core-shell-structure NFs composed of PPy NFs have good plasticity and mechanical properties, providing perfect ductility and mechanical properties for better extraction of trace sulfated azo dyes from aqueous solution. Core-shell-structured NFs can improve the recovery and repeatability of sulfated azo dyes, and PPy NFs not only extract target compounds but also effectively remove interference. Simple, fast, sensitive, and uninterrupted, this method can provide a good alternative tool for the determination of contaminants in water samples. Abedalwafa et al. made aptamer immobilized electrospun-NF membranes (A-

NFMs) with signal probes (DNA-conjugated gold nanoparticles (AuNPs)) combined with a colorimetric measurement of kanamycin (KMC) to prepare a portable biosensor [176]. The A-NFMs were modified with the complementary single-stranded DNA (cDNA) of the KMC aptamer-coupled AuNP (cDNA @ Au) as a colorimetric agent. The prepared colorimetric sensor finally can visually observe the resulting color changes with good selectivity and applicability. Compared to the traditional two-dimensional planar film, the special structure of electrospun NFs, due to their versatility, high porosity, and specific surface area, can improve its sensitivity and responsiveness; they not only have an excellent sensing performance but also a good adsorption performance and can continuously analyze trace pollutants in polluted water, thus making them more suitable for water detection.

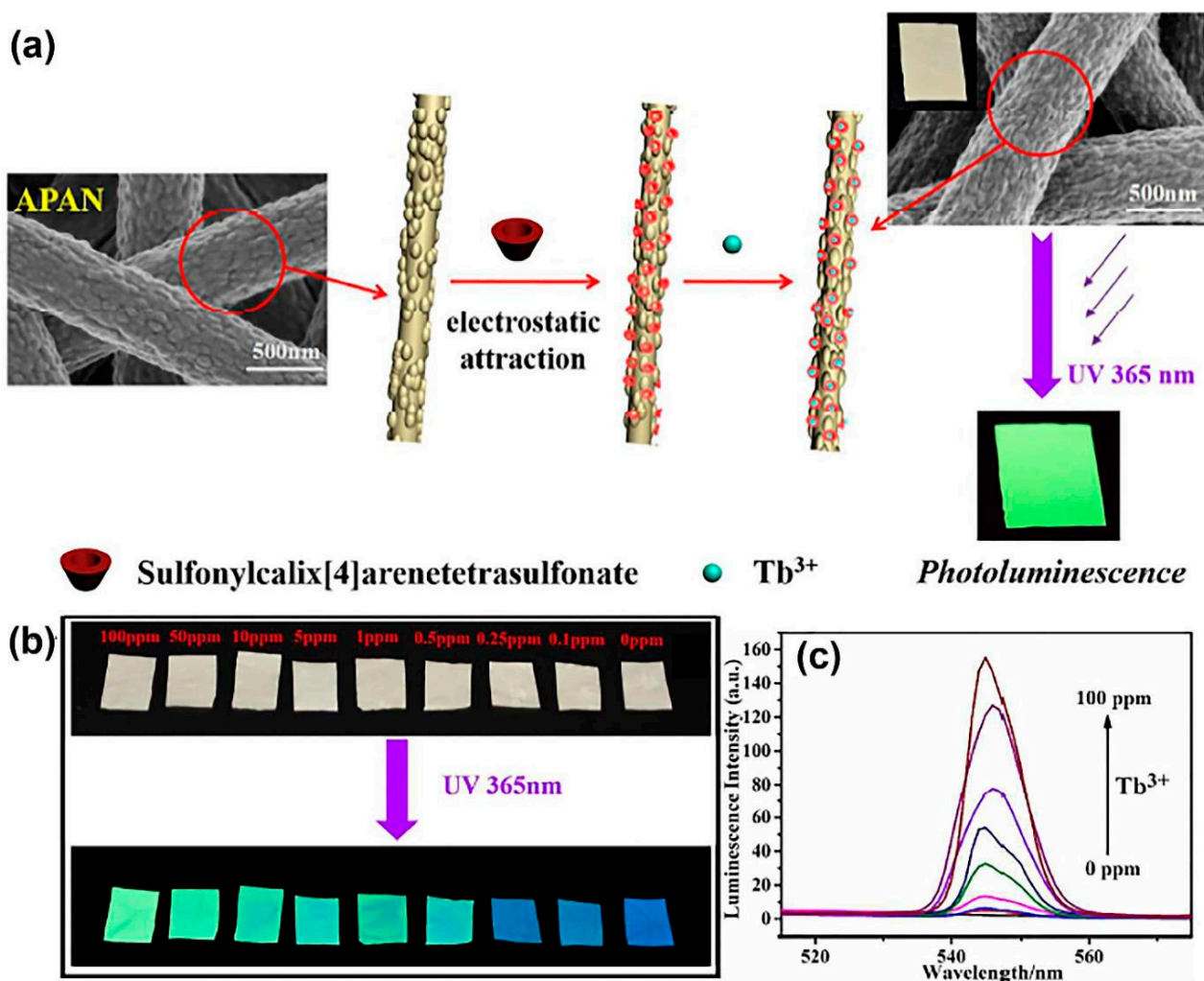


Figure 5. Electrospun-NFs-based chemosensors for water pollutant. (a) Preparation procedure and photoluminescent behavior of sulfonylcalix[4]arene-functionalized APAN nanofibrous for the adsorptive removal of Tb^{3+} ions. (b) Photographs of NFs after immersing into Tb^{3+} aqueous solutions (0–100 ppm). (c) Fluorescence spectra of NFs (reproduced with permission from [173], copyright © 2018, Royal Society of Chemistry).

4.2. Gas Pollutant

Toxic gases in the environment can affect the human respiratory system and even contribute to global warming, making the monitoring of polluting gases a crucial aspect of air quality management. A gas sensor is a device that provides a signal in response to a specific target gas, and gas-sensing technology has made significant progress in environmental

testing, enabling the effective detection of air pollutants. Gas sensors are often required to detect toxic, highly corrosive, and irritating gases, such as inorganic and organic gases, in environmental pollution detection. Electrospinning technology can be used to fabricate NF-based gas chemosensors that enhance sensing performance, improve chemical and physical properties, increase specific surface area and interaction sites, and enhance the diffusion coefficient. Compared to other types of nano-based sensors, this sensing system can improve the sensitivity to gases and can be combined with other nanomaterials to enhance electrospinning-based sensing parameters. NF-based chemosensors can detect a variety of analytes in different states without interference. However, the response time during gas sensing may be limited due to factors such as slow gas diffusion, the adsorption characteristics, and the working environment, which can affect the real-time responsiveness of analytes [177]. Terra et al. used p-electron conjugation in conjugated polymers to design highly fluorescent PMMA/polyfluorene (PFO) electrospinning NFs for optical gas sensing through luminescence quenching [178]. These NFs can detect different volatile organic compounds (VOCs), such as chloroform, toluene, acetone, and ethanol. When the NFs are exposed to certain vapors, they undergo a conformational change from the glass phase to B phase under VOCs, causing fluorescence quenching that can be analyzed. The flexible morphological structures of PMMA/PFO NFs constructed by electrospinning provide large surface-to-volume ratios, greatly enhancing chemical functionalization and interaction with target analytes (VOCs), which can improve the sensor's performance (Figure 6A). Han et al. prepared a sensor based on $\text{In}_2\text{O}_3/\text{ZnO}$ yolk-shell NFs [179]. These NFs can improve the gas-sensing performance due to their heterojunction effect, which enhances the efficiency of photogenerated charge separation, increases reaction sites, and enhances gas adsorption. The $\text{In}_2\text{O}_3/\text{ZnO}$ -sensing material with the YS heterostructure was synthesized using the traditional electrospinning method, resulting in an ordered semiconductor heterostructure with a hollow structure (Figure 6B). The hollow structure and abundant pores significantly increase the inward diffusion rate of the gas, resulting in more active sites, which is conducive to charge separation and gas transfer. The increase of adsorption sites of hollow structures directly enhances the surface reaction involved in the gas to be measured, thereby showing a high sensing performance. The fast detection response and complete recovery characteristics of the sensor greatly improve its sensing performance. Ngoensawat et al. prepared 2,5-dibromo-3,4-ethylenedioxythiophene (DBEDOT), poly(vinyl alcohol) (PVA), and silver nanoparticles (AgNPs) in PEDOT/PVA/AgNPs composite fibers by emulsion electrospinning [180]. PEDOT/PVA/AgNPs composite fibers detected heavy metal ions (Zn(II) , Cd(II) , and Pb(II)) in analytes by positive wave anode stripping voltammetry (SWASV). It was demonstrated that electrospinning combined with solid-state polymerization (SSP) is a simple, catalyst-free, and complex instrument-free method for the preparation of PEDOT-based electrochemical analysis platforms (Figure 6C). Deng et al. prepared the electrospun core-shell multiwalled carbon nanotubes (MWCNTs)/gelatin-hemoglobin (Hb) nanobelts on an electrode surface [181]. The electrocatalytic activity of the nanobelts toward the reduction of H_2O_2 is improved by protein adsorption, which enhances electron-transfer kinetics. The core-shell structure of the nanobelts, with MWCNTs providing conductivity and the gelatin-Hb shell conferring biocompatibility and protein adsorption capability, plays a critical role in this process. The preparation method based on electrospinning can be directly deposited on the electrode surface, adjustable-size NFs can be prepared at the specified deposition position, and the fibers can be adapted to the auto-preconcentration of the analyte on the electrode, thereby improving the sensitivity of electrochemical detection of real trace sample analytes.

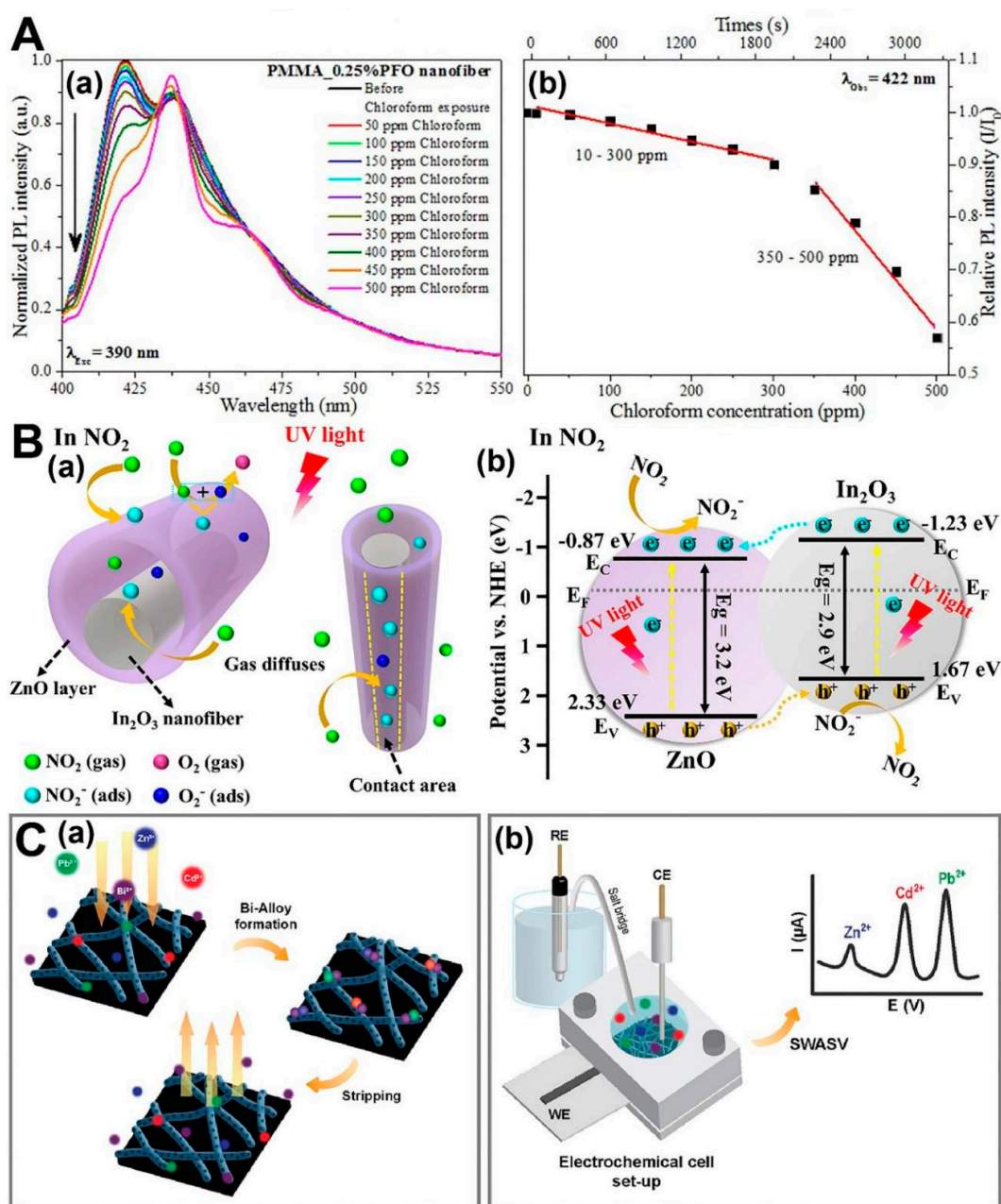


Figure 6. Electropun-NFs-based chemosensors for gas pollutant. (A) PL spectra. (a) PMMA_0.25%PFO NF exposition to chloroform vapor; it was excited at 390 nm. (b) The dependence of the emission intensity as function of chloroform concentration for PMMA_0.25%PFO NF (monitored at 420 nm) (reproduced with permission from [178], copyright © 2017, Wiley Periodicals). (B) Schematic diagrams of (a) NO_2 detection process, (b) $\text{In}_2\text{O}_3/\text{ZnO}$ heterojunctions, and corresponding energy band diagram (reproduced with permission from [179], copyright © 2021, Elsevier). (C) The PEDOT/PVA/AgNPs-fibers-modified SPCE preparation. (a) Bi-alloy formation on electrode surface, followed by stripping. (b) Electrochemical detection of heavy metal ions via SWASV (reproduced with permission from [180], copyright © 2022, Elsevier).

4.3. Soil Pollutant

Soil pollution caused by agricultural production and industrial development has become an increasing environmental concern. Due to the pollution caused by pollutants, the self-purification ability of the soil itself will change in space and time. Therefore, a continuous and accurate temporal and spatial monitoring of the physical properties of the soil is

required. However, compared with water- and air-pollution monitoring, the development of soil-sensing monitoring is not fast. The challenges of soil-sensing monitoring include the difficulties in sample separation and treatment compared to water- and air-pollution monitoring. Dielectric assays can be useful for characterizing soil pollutants by relying on information about the dielectric properties of contaminated soil. Electromagnetic methods can measure the soil dielectric properties and determine the substances included in the dielectric properties. In addition, biosensors, particularly enzyme biosensors, can be highly specific and sensitive to analytes and can be used to systematically evaluate contaminated soil based on the fluctuation of enzyme activity detected in the presence of contaminants. Furthermore, NFs can act as a catalytic medium due to their high specific surface area and active site characteristics, thus improving the conductivity and catalytic activity and enabling high-precision detection of soil pollutants. Jin et al. prepared a ratiometric fluorescent probe for the detection of copper ions (Cu^{2+}), using a combination of electrospinning, strip testing, and hydrogel-encapsulation techniques [182]. The probe was composed of ATP and a fluorophore, which exhibited a reversible response to Cu^{2+} ions. The probe was able to detect Cu^{2+} ions with high sensitivity and selectivity in living cells and in soil samples, making it a useful tool for environmental safety assessment. Electrospinning has the potential to be a powerful tool for developing novel probes and sensors for various applications, including environmental monitoring and biomedical diagnostics (Figure 7). Srinivasan et al. developed a composite electrode by using copper and reduced graphene oxide (Cu-rGO) NFs for the ultralow-level detection of the pesticide imidacloprid (IMD) in soil, with high catalytic activity provided by the combination of NFs with redox copper and rGO [183]. The use of electrospun composite NFs provides necessary chemical sensing and electrocatalytic activity for the accurate detection of soil pollutants in real time. Therefore, the composite NFs prepared through the electrospinning technique offer both the chemical sensing and electrocatalytic activity necessary for soil pollutant detection.

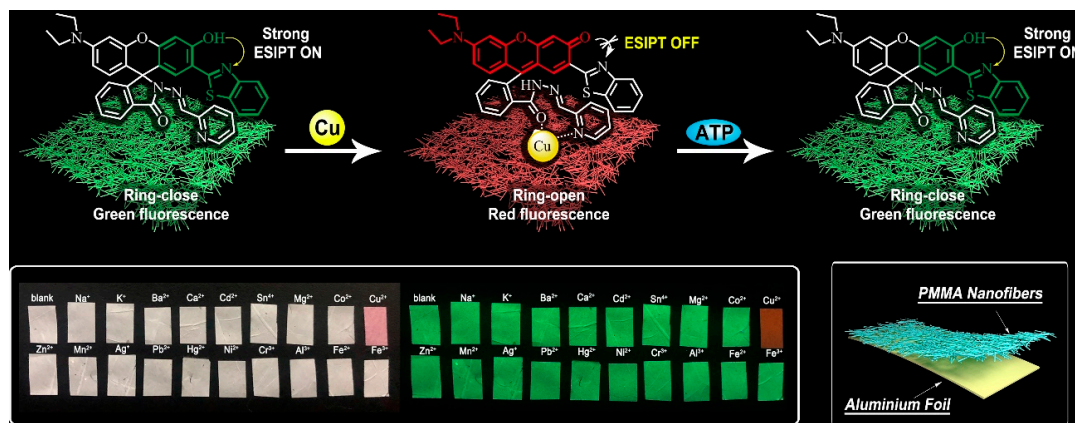


Figure 7. Schematic illustration of a ratiometric fluorescent sensing platform that uses a probe-doped PMMA material for the specific and visual detection of Cu^{2+} and ATP sequentially, with photographs of the nanofibers exposed to different metal ions that confirm the selectivity of the platform (reproduced with permission from [182], copyright © 2020, Elsevier).

From the above discussion, it can be seen that the NFs prepared via the electrospinning process can effectively solve the manufacturing problems of such sensors due to their unique surface morphology and a variety of nanostructures, such as the core-shell structure, Janus structure, tertiary core-shell/Janus structure, hollow structure, porous structure, etc. Both the sensing methods used and the multiple structural NFs can play different roles in detecting various analytes in different states. An example includes optical sensors that detect solutions and gases with less interference and that can achieve color change by adding chromogenic agents, MOF, QDs, and other optically active functional groups to NFs.

However, in soil detection, the sensing characteristics of NFs, such as the response time, may be limited due to the slow diffusion and adsorption of analytes, which reduces the interaction time between the analyte and reactant and limits the applicability of the analyte. To overcome this limitation, NFs with different structures can be utilized to improve the active adsorption site and shorten the response time, thus enhancing the real-time reliability and stability of detection (Table 1). Currently, electrospun nanofiber-based sensors are mostly prepared by single and coaxial electrospinning to obtain nanofibers with uniaxial, core-shell, porous, and hollow structures. The good electron-transfer characteristics of various nanostructured NFs enable them to have excellent electrocatalytic activity, including sensitivity, selectivity, stability, repeatability, and multiplexing capabilities. Electrospinning sensors are effective at adsorbing and sensing a range of analytes, with low detection limits and fast response times. With the advancement of electrospinning technology, the unique NF structure is improving the sensing performance of chemosensors.

Table 1. Electrospun-NFs-based chemosensors for environmental pollution detections.

Detection Method	Materials	Structure	Target Analyte	Linear Range	LOD	Application Area	Ref.
Electrochemical	NH ₂ -MIL-101(Fe)/CNF@AuNPs	Single	Tetracycline	0.1–10 ⁵ nM	0.01 nM	Water	[41]
Electrochemical	CuO/PANI hybrid NFs	Hollow	H ₂ O ₂	0.005–9.255 mM	0.11 mM	–	[111]
Electrochemical	CoFe ₂ Se ₄ /PCF	Porous	HQ	0.5–200 μM	0.13 μM	Water	[113]
			CC	0.5–190 μM	0.15 μM		
Fluorescent	3D porous fluorescent lignin	Porous	RS	5–350 μM	1.36 μM	Water	[159]
			Hexavalent chromium	15–200 mg/L	11.2 mg/L		
Colorimetric	Br-PADAP/CA NFs	Single	Uranyl	0–500 ppb	50 ppb	Water	[170]
Fluorescent	Sulfonylcalix-NFM	Porous	Terbium(III) ions	0.1–100 ppm	0.5 ppm	Water	[173]
Colorimetric	cDNA@Au/GA-CA NFM	Single	Kanamycin	2.5–80 nM	2.5 nM	Water	[176]
Fluorescent	PMMA/PFO NFs	Single	Chloroform	10–300 ppm	47.9 ppm	Air	[178]
Electrochemical	PEDOT/PVA/AgNPs NFs	Single	Zn(II)	350–500 ppm	15.4 ppm		
			Cd(II)	10–80 ppb	6 ppb	–	[180]
			Pb(II)	10–80 ppb	3 ppb		
Electrochemical	MWCNTs/gelatin-Hb nanobelts	Core-shell	H ₂ O ₂	5.0 × 10 ^{−6} –55 × 10 ^{−6} mol/L	0.0293 μmol/L	–	[181]
Fluorescent	RB/PMMA NFs	Single	Copper ion	0.0–10 μM	0.11 μM	Soil	[182]
			ATP	0.0–10 μM	0.08 μM		

5. Conclusions and Perspectives

Electrospinning can generate a high-specific-surface-area and three-dimensional porous meshes that can serve as chemosensors and be capable of pollution treatment due to their unique structure and multistage processing [169,184,185]. Electrospinning has developed rapidly in the direction of nanotechnology, developing toward microtechnology, complex nanostructures/nanodevices, and various nanoarrays, and has shown its application advantages in various scientific fields. This paper provides an overview of the vision recognition sensing platform and rapid electron transfer sensing technology based on electrospinning with different structures. Multi-fluid electrospinning has powerful capabilities, among which multi-component core-shell/Janus-structure NFs have a high Young's modulus and tensile strength, which can achieve multistage redox reactions or have multiplexed detection capabilities. The adsorption and water stability of composite porous structure NFs provide greater possibilities for the preparation of flexible sensors, and their higher S/N ratio provides more active sites for optical sensing, so that analyte diffusion can promote and accelerate the interaction between analyte and identification sites. Moreover, hollow-structure NFs with high surface area can improve capacitance to shorten the response time during sensing. This paper summarizes the research progress of sensing NFs in environmental monitoring and points out the applicability of multi-fluid electrospinning technology in multicomponent chemical sensing. The chemosensor for the

electrospinning preparation addresses the disadvantages of spectral analysis equipment, while the fiber properties exhibiting outstanding bending and expansion properties do not affect the conductive properties of the electrochemical sensor. Using electrochemical and optical sensing can enable field real-time detection and high sensing performance, with simple operation and the ability to detect different substances at the same time. Therefore, based on the development of electrospinning, with electrospinning nanostructures as a strong support platform, it is increasingly possible to detect environmental pollutants, and new nanostructures can be manufactured in a simple way, which has great prospects in the manufacturing of large-scale chemical sensors.

Chemosensors contribute significantly to a cleaner and greener environment in the detection of environmental pollutants (in air, water, and soil, including other pollution, such as sound, light, and electromagnetic pollution), and the ongoing chemical-sensing technology has strong future potential. The improvement of sensors requires new chemically synthesized functional substances, new nanostructured materials, ease of application, and functional integration or synergy. The high porosity of electrospun NFs and the multiple adsorption sites formed by large specific surface area also make them have a good adsorption performance, and by combining the adsorption and degradation characteristics of NFs for pollutants, dual-functional environmental-pollution-sensing detection and adsorption degradation treatment are realized. Electrospinning plays an important role in the synthesis of novel nanomaterials by combining materials such as NPs, QDs, and MOFs. This process enhances electrochemical properties through reversible redox reactions, providing greater potential for the next generation of optoelectronic sensing. Due to its unique structure and multi-fluid process, electrospinning technology can prepare new nanomaterials with a multistage structure, adjustable form, high flexibility, and composite functional properties. This makes nanofiber-based sensors have excellent synergy to realize application and function integration, and the simple preparation method enables the repeatability of chemosensors at low cost, which is suitable for industrialization (Figure 8). The use of natural sources in electrospinning NFs has also realized the development of green materials, which is suitable for the development of environmentally protective and pollution-free environmental detection equipment. This provides a new direction for the next improvement of sensors. Furthermore, the brand-new knowledge and strategies from other subdisciplines of chemistry can be imitated or borrowed for developing new types of chemosensors with electrospinning as an integration tool [186–193].

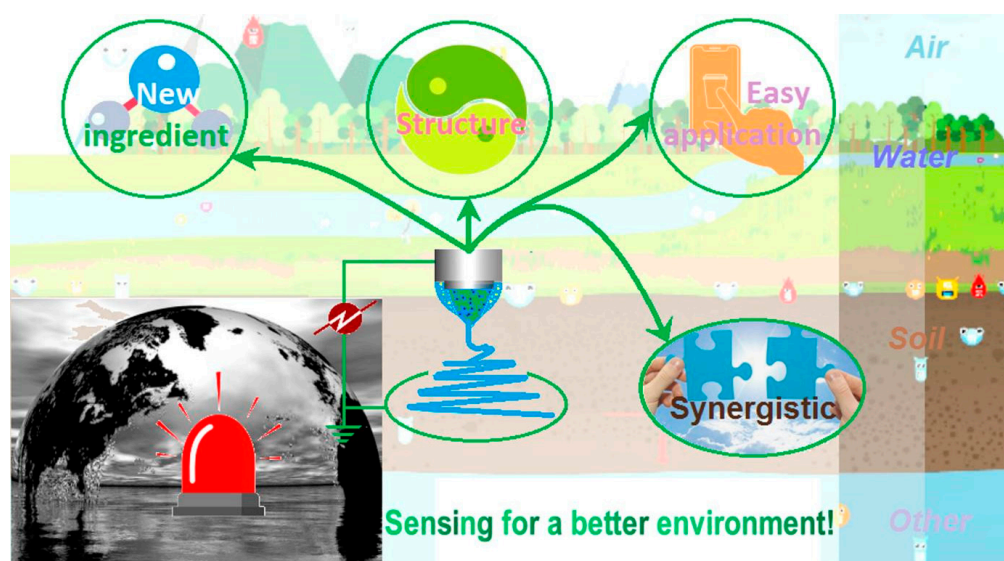


Figure 8. Application prospect of electrospinning technology in the improvement of detection of environmental chemosensors.

Author Contributions: Conceptualization, Y.D. and D.-G.Y.; methodology, Y.D.; writing—original draft preparation, Y.D.; writing—review and editing, D.-G.Y. and T.Y.; visualization, Y.D.; supervision, D.-G.Y.; project administration, D.-G.Y.; funding acquisition, D.-G.Y. and T.Y. All authors have read and agreed to the published version of the manuscript.

Funding: This investigation was financially supported by the Medical Engineering Cross Project between the University of Shanghai for Science and Technology and the Naval Medical University (No. 2020-RZ05); the Shanghai Natural Science Foundation (No. 20ZR1439000); and the Macao Polytechnic University Research Fund (RP/FCSD-01/2023).

Institutional Review Board Statement: Not applicable.

Informed Consent Statement: Not applicable.

Data Availability Statement: The data supporting the findings of this manuscript are available from the corresponding authors upon reasonable.

Acknowledgments: Chenqi Li and Ruiliang Ge are appreciated for their help during the preparation of this review.

Conflicts of Interest: The authors declare no conflict of interest.

References

1. Dey, T.K.; Uddin, M.E.; Jamal, M. Detection and Removal of Microplastics in Wastewater: Evolution and Impact. *Environ. Sci. Pollut. Res.* **2021**, *28*, 16925–16947. [[CrossRef](#)]
2. Wayman, C.; Niemann, H. The Fate of Plastic in the Ocean Environment—A Minireview. *Environ. Sci.-Process. Impacts* **2021**, *23*, 198–212. [[CrossRef](#)] [[PubMed](#)]
3. Tullo, E.; Finzi, A.; Guarino, M. Review: Environmental Impact of Livestock Farming and Precision Livestock Farming as a Mitigation Strategy. *Sci. Total Environ.* **2019**, *650*, 2751–2760. [[CrossRef](#)]
4. Mai, L.; Bao, L.-J.; Shi, L.; Wong, C.S.; Zeng, E.Y. A Review of Methods for Measuring Microplastics in Aquatic Environments. *Environ. Sci. Pollut. Res.* **2018**, *25*, 11319–11332. [[CrossRef](#)]
5. Yuan, Z.; Nag, R.; Cummins, E. Human Health Concerns Regarding Microplastics in the Aquatic Environment—From Marine to Food Systems. *Sci. Total Environ.* **2022**, *823*, 153730. [[CrossRef](#)]
6. Smith, D.M.; Scaife, A.A.; Eade, R.; Athanasiadis, P.; Bellucci, A.; Bethke, I.; Bilbao, R.; Borchert, L.F.; Caron, L.-P.; Counillon, F.; et al. North Atlantic Climate Far More Predictable than Models Imply. *Nature* **2020**, *583*, 796–800. [[CrossRef](#)]
7. Liu, X.; Reddi, K.; Elgowainy, A.; Lohse-Busch, H.; Wang, M.; Rustagi, N. Comparison of Well-to-Wheels Energy Use and Emissions of a Hydrogen Fuel Cell Electric Vehicle Relative to a Conventional Gasoline-Powered Internal Combustion Engine Vehicle. *Int. J. Hydrogen Energy* **2020**, *45*, 972–983. [[CrossRef](#)]
8. Singh, S.; Kumar, V.; Chauhan, A.; Datta, S.; Wani, A.B.; Singh, N.; Singh, J. Toxicity, Degradation and Analysis of the Herbicide Atrazine. *Environ. Chem. Lett.* **2018**, *16*, 211–237. [[CrossRef](#)]
9. Li, H.-Y.; Zhao, S.-N.; Zang, S.-Q.; Li, J. Functional Metal-Organic Frameworks as Effective Sensors of Gases and Volatile Compounds. *Chem. Soc. Rev.* **2020**, *49*, 6364–6401. [[CrossRef](#)] [[PubMed](#)]
10. Le, V.T.; Vasseghian, Y.; Doan, V.D.; Nguyen, T.T.T.; Vo, T.-T.T.; Do, H.H.; Vu, K.B.; Vu, Q.H.; Lam, T.D.; Tran, V.A. Flexible and High-Sensitivity Sensor Based on Ti₃C₂-MoS₂ MXene Composite for the Detection of Toxic Gases. *Chemosphere* **2022**, *291*, 133025. [[CrossRef](#)]
11. Liu, J.; Zhang, L.; Cheng, B.; Fan, J.; Yu, J. A High-Response Formaldehyde Sensor Based on Fibrous Ag-ZnO/In₂O₃ with Multi-Level Heterojunctions. *J. Hazard. Mater.* **2021**, *413*, 125352. [[CrossRef](#)] [[PubMed](#)]
12. He, S.; Zhu, B.; Jiang, X.; Han, G.; Li, S.; Lau, C.H.; Wu, Y.; Zhang, Y.; Shao, L. Symbiosis-Inspired de Novo Synthesis of Ultrahigh MOF Growth Mixed Matrix Membranes for Sustainable Carbon Capture. *Proc. Natl. Acad. Sci. USA* **2022**, *119*, e2114964119. [[CrossRef](#)] [[PubMed](#)]
13. Liu, L.; Meng, W.-K.; Li, L.; Xu, G.-J.; Wang, X.; Chen, L.-Z.; Wang, M.-L.; Lin, J.-M.; Zhao, R.-S. Facile Room-Temperature Synthesis of a Spherical Mesoporous Covalent Organic Framework for Ultrasensitive Solid-Phase Microextraction of Phenols Prior to Gas Chromatography-Tandem Mass Spectrometry. *Chem. Eng. J.* **2019**, *369*, 920–927. [[CrossRef](#)]
14. Liu, L.; Meng, W.-K.; Zhou, Y.-S.; Wang, X.; Xu, G.-J.; Wang, M.-L.; Lin, J.-M.; Zhao, R.-S. Beta-Ketoenamine-Linked Covalent Organic Framework Coating for Ultra-High-Performance Solid-Phase Microextraction of Polybrominated Diphenyl Ethers from Environmental Samples. *Chem. Eng. J.* **2019**, *356*, 926–933. [[CrossRef](#)]
15. Zhang, Z.-H.; Zhang, J.-W.; Cao, C.-F.; Guo, K.-Y.; Zhao, L.; Zhang, G.-D.; Gao, J.-F.; Tang, L.-C. Temperature-Responsive Resistance Sensitivity Controlled by L-Ascorbic Acid and Silane Co-Functionalization in Flame-Retardant GO Network for Efficient Fire Early-Warning Response. *Chem. Eng. J.* **2020**, *386*, 123894. [[CrossRef](#)]
16. Tang, W.; Wang, D.; Wang, J.; Wu, Z.; Li, L.; Huang, M.; Xu, S.; Yan, D. Pyrethroid Pesticide Residues in the Global Environment: An Overview. *Chemosphere* **2018**, *191*, 990–1007. [[CrossRef](#)]

17. van den Berg, N.J.; van Soest, H.L.; Hof, A.F.; den Elzen, M.G.J.; van Vuuren, D.P.; Chen, W.; Drouet, L.; Emmerling, J.; Fujimori, S.; Hoehne, N.; et al. Implications of Various Effort-Sharing Approaches for National Carbon Budgets and Emission Pathways. *Clim. Chang.* **2020**, *162*, 1805–1822. [[CrossRef](#)]
18. Kumar, R.; Sharma, P.; Manna, C.; Jain, M. Abundance, Interaction, Ingestion, Ecological Concerns, and Mitigation Policies of Microplastic Pollution in Riverine Ecosystem: A Review. *Sci. Total Environ.* **2021**, *782*, 146695. [[CrossRef](#)]
19. Kubra, K.T.; Salman, M.S.; Znad, H.; Hasan, M.N. Efficient Encapsulation of Toxic Dye from Wastewater Using Biodegradable Polymeric Adsorbent. *J. Mol. Liq.* **2021**, *329*, 115541. [[CrossRef](#)]
20. Pang, X.; Skillen, N.; Gunaratne, N.; Rooney, D.W.; Robertson, P.K.J. Removal of Phthalates from Aqueous Solution by Semiconductor Photocatalysis: A Review. *J. Hazard. Mater.* **2021**, *402*, 123461. [[CrossRef](#)]
21. Wang, Y.; Zhu, G.; Li, M.; Singh, R.; Marques, C.; Min, R.; Kaushik, B.K.; Zhang, B.; Jha, R.; Kumar, S. Water Pollutants P-Cresol Detection Based on Au-ZnO Nanoparticles Modified Tapered Optical Fiber. *Ieee Trans. Nanobiosci.* **2021**, *20*, 377–384. [[CrossRef](#)]
22. Fan, L.; Zhao, D.; Li, B.; Wang, F.; Deng, Y.; Peng, Y.; Wang, X.; Zhang, X. Luminescent Binuclear Zinc(II) Organic Framework as Bifunctional Water-Stable Chemosensor for Efficient Detection of Antibiotics and Cr(VI) Anions in Water. *Spectrochim. Acta Part-Mol. Biomol. Spectrosc.* **2022**, *264*, 120232. [[CrossRef](#)]
23. Wagner, M.; Lin, K.-Y.A.; Oh, W.-D.; Lisak, G. Metal-Organic Frameworks for Pesticidal Persistent Organic Pollutants Detection and Adsorption—A Mini Review. *J. Hazard. Mater.* **2021**, *413*, 125325. [[CrossRef](#)]
24. Wang, Y.; Zhang, L.; Han, X.; Zhang, L.; Wang, X.; Chen, L. Fluorescent Probe for Mercury Ion Imaging Analysis: Strategies and Applications. *Chem. Eng. J.* **2021**, *406*, 127166. [[CrossRef](#)]
25. Qian, L.; Durairaj, S.; Prins, S.; Chen, A. Nanomaterial-Based Electrochemical Sensors and Biosensors for the Detection of Pharmaceutical Compounds. *Biosens. Bioelectron.* **2021**, *175*, 112836. [[CrossRef](#)] [[PubMed](#)]
26. Zhang, Y.; Sun, A.; Xiong, M.; Macharia, D.K.; Liu, J.; Chen, Z.; Li, M.; Zhang, L. TiO₂/BiOI p-n Junction-Decorated Carbon Fibers as Weavable Photocatalyst with UV-Vis Photoresponsive for Efficiently Degrading Various Pollutants. *Chem. Eng. J.* **2021**, *415*, 129019. [[CrossRef](#)]
27. Balram, D.; Lian, K.-Y.; Sebastian, N.; Al-Mubaddel, F.S.; Noman, M.T. Bi-Functional Renewable Biopolymer Wrapped CNFs/Ag Doped Spinel Cobalt Oxide as a Sensitive Platform for Highly Toxic Nitroaromatic Compound Detection and Degradation. *Chemosphere* **2022**, *291*, 132998. [[CrossRef](#)] [[PubMed](#)]
28. Guo, J.-J.; Huang, X.-P.; Xiang, L.; Wang, Y.-Z.; Li, Y.-W.; Li, H.; Cai, Q.-Y.; Mo, C.-H.; Wong, M.-H. Source, Migration and Toxicology of Microplastics in Soil. *Environ. Int.* **2020**, *137*, 105263. [[CrossRef](#)] [[PubMed](#)]
29. Yaseen, Z.M. The next Generation of Soil and Water Bodies Heavy Metals Prediction and Detection: New Expert System Based Edge Cloud Server and Federated Learning Technology. *Environ. Pollut.* **2022**, *313*, 120081. [[CrossRef](#)]
30. Lu, Y.; Liang, X.; Niyungeko, C.; Zhou, J.; Xu, J.; Tian, G. A Review of the Identification and Detection of Heavy Metal Ions in the Environment by Voltammetry. *Talanta* **2018**, *178*, 324–338. [[CrossRef](#)]
31. He, S.; Wei, Y.; Yang, C.; He, Z. Interactions of Microplastics and Soil Pollutants in Soil-Plant Systems. *Environ. Pollut.* **2022**, *315*, 120357. [[CrossRef](#)]
32. Tajik, S.; Beitollahi, H.; Nejad, F.G.; Dourandish, Z.; Khalilzadeh, M.A.; Jang, H.W.; Venditti, R.A.; Varma, R.S.; Shokouhimehr, M. Recent Developments in Polymer Nanocomposite-Based Electrochemical Sensors for Detecting Environmental Pollutants. *Ind. Eng. Chem. Res.* **2021**, *60*, 1112–1136. [[CrossRef](#)] [[PubMed](#)]
33. Mao, C.; Zhao, H.; Ye, H.; Zhao, L. Be-Original Break New Ground: Fluorescence Sensing of Humic Acid in Natural Water and Soil by Pitaya Seed Carbon Dots. *Spectrochim. Acta Part-Mol. Biomol. Spectrosc.* **2023**, *286*, 121950. [[CrossRef](#)] [[PubMed](#)]
34. Tripathy, A.K.; Tripathy, S.K.; Sundaray, M. An Ultra-Sensitive Optical Sensor Based on Agarose Coated Microscopic Sphere to Detect Cu²⁺ ion in Soil. *Comput. Electron. Agric.* **2022**, *202*, 107424. [[CrossRef](#)]
35. Huang, D.; Gao, L.; Zheng, M.; Qiao, L.; Xu, C.; Wang, K.; Wang, S. Screening Organic Contaminants in Soil by Two-Dimensional Gas Chromatography High-Resolution Time-of-Flight Mass Spectrometry: A Non-Target Analysis Strategy and Contaminated Area Case Study. *Environ. Res.* **2022**, *205*, 112420. [[CrossRef](#)]
36. Shi, T.; Chen, Y.; Liu, Y.; Wu, G. Visible and Near-Infrared Reflectance Spectroscopy—An Alternative for Monitoring Soil Contamination by Heavy Metals. *J. Hazard. Mater.* **2014**, *265*, 166–176. [[CrossRef](#)]
37. Ivleva, N.P. Chemical Analysis of Microplastics and Nanoplastics: Challenges, Advanced Methods, and Perspectives. *Chem. Rev.* **2021**, *121*, 11886–11936. [[CrossRef](#)]
38. Kaushal, J.; Khatri, M.; Arya, S.K. A Treatise on Organophosphate Pesticide Pollution: Current Strategies and Advancements in Their Environmental Degradation and Elimination. *Ecotoxicol. Environ. Saf.* **2021**, *207*, 111483. [[CrossRef](#)] [[PubMed](#)]
39. Cheng, J.; Huang, X.; Chen, L.; Yan, L.; Zhu, F.; Li, H. Fabrication of Molecularly Imprinted Nanochannel Membrane for Ultrasensitive Electrochemical Detection of Triphenyl Phosphate. *Anal. Chim. Acta* **2022**, *1192*, 339374. [[CrossRef](#)]
40. Rebelo, P.; Costa-Rama, E.; Seguro, I.; Pacheco, J.G.; Nouws, H.P.A.; Cordeiro, M.N.D.S.; Delerue-Matos, C. Molecularly Imprinted Polymer-Based Electrochemical Sensors for Environmental Analysis. *Biosens. Bioelectron.* **2021**, *172*, 112719. [[CrossRef](#)]
41. Song, J.; Huang, M.; Lin, X.; Li, S.F.Y.; Jiang, N.; Liu, Y.; Guo, H.; Li, Y. Novel Fe-Based Metal-Organic Framework (MOF) Modified Carbon Nanofiber as a Highly Selective and Sensitive Electrochemical Sensor for Tetracycline Detection. *Chem. Eng. J.* **2022**, *427*, 130913. [[CrossRef](#)]
42. Chen, G.; Bai, W.; Jin, Y.; Zheng, J. Fluorescence and Electrochemical Assay for Bimodal Detection of Lead Ions Based on Metal-Organic Framework Nanosheets. *Talanta* **2021**, *232*, 122405. [[CrossRef](#)]

43. Tang, X.; Su, R.; Luo, H.; Zhao, Y.; Feng, L.; Chen, J. Colorimetric Detection of Aflatoxin B-1 by Using Smartphone-Assisted Microfluidic Paper-Based Analytical Devices. *Food Control*. **2022**, *132*, 108497. [[CrossRef](#)]
44. Chen, Z.; Zhang, Z.; Qi, J.; You, J.; Ma, J.; Chen, L. Colorimetric Detection of Heavy Metal Ions with Various Chromogenic Materials: Strategies and Applications. *J. Hazard. Mater.* **2023**, *441*, 129889. [[CrossRef](#)] [[PubMed](#)]
45. Qiu, Y.; Qu, K. Binary Organic-Inorganic Nanocomposite of Polyaniline-MnO₂ for Non-Enzymatic Electrochemical Detection of Environmental Pollutant Nitrite. *Environ. Res.* **2022**, *214*, 114066. [[CrossRef](#)] [[PubMed](#)]
46. Xu, L.; Abd El-Aty, A.M.; Eun, J.-B.; Shim, J.-H.; Zhao, J.; Lei, X.; Gao, S.; She, Y.; Jin, F.; Wang, J.; et al. Recent Advances in Rapid Detection Techniques for Pesticide Residue: A Review. *J. Agric. Food Chem.* **2022**, *70*, 13093–13117. [[CrossRef](#)] [[PubMed](#)]
47. Xie, X.; Gao, N.; Zhu, L.; Hunter, M.; Chen, S.; Zang, L. PEDOT:PSS/PEDOT Film Chemiresistive Sensors for Hydrogen Peroxide Vapor Detection under Ambient Conditions. *Chemosensors* **2023**, *11*, 124. [[CrossRef](#)]
48. Berhanu, A.L.; Gaurav; Mohiuddin, I.; Malik, A.K.; Aulakh, J.S.; Kumar, V.; Kim, K.-H. A Review of the Applications of Schiff Bases as Optical Chemical Sensors. *Trac-Trends Anal. Chem.* **2019**, *116*, 74–91. [[CrossRef](#)]
49. Kulandaivel, S.; Lo, W.-C.; Lin, C.-H.; Yeh, Y.-C. Cu-PyC MOF with Oxidoreductase-like Catalytic Activity Boosting Colorimetric Detection of Cr(VI) on Paper. *Anal. Chim. Acta* **2022**, *1227*, 340335. [[CrossRef](#)]
50. Aijaz, A.; Raja, D.A.; Khan, F.-A.; Berek, J.; Malik, M.I. A Silver Nanoparticles-Based Selective and Sensitive Colorimetric Assay for Ciprofloxacin in Biological, Environmental, and Commercial Samples. *Chemosensors* **2023**, *11*, 91. [[CrossRef](#)]
51. Rahman, S.; Bozal-Palabiyik, B.; Unal, D.N.; Erkmen, C.; Siddiq, M.; Shah, A.; Uslu, B. Molecularly Imprinted Polymers (MIPs) Combined with Nanomaterials as Electrochemical Sensing Applications for Environmental Pollutants. *Trends Environ. Anal. Chem.* **2022**, *36*, e00176. [[CrossRef](#)]
52. Zhang, X.; Hao, X.; Zhai, Z.; Wang, J.; Li, H.; Sun, Y.; Qin, Y.; Niu, B.; Li, C. Flexible H₂S Sensors: Fabricated by Growing NO₂-UiO-66 on Electrospun Nanofibers for Detecting Ultralow Concentration H₂S. *Appl. Surf. Sci.* **2022**, *573*, 151446. [[CrossRef](#)]
53. Lazarević-Pašti, T.; Tasić, T.; Milanković, V.; Potkonjak, N. Molecularly Imprinted Plasmonic-Based Sensors for Environmental Contaminants—Current State and Future Perspectives. *Chemosensors* **2023**, *11*, 35. [[CrossRef](#)]
54. Tan, S.; Wang, Q.; Tan, Q.; Zhao, S.; Huang, L.; Wang, B.; Song, X.; Lan, M. Ratiometric Fluorescence Probe Based on Deep-Red Emissive CdTe Quantum Dots and Eu³⁺ Hybrid for Oxytetracycline Detection. *Chemosensors* **2023**, *11*, 62. [[CrossRef](#)]
55. Tay, Y.Y.; Lin, X.H.; Li, S.F.Y. Nanogel for Selective Recognition of Nanoparticles in Water Samples. *Chemosensors* **2023**, *11*, 72. [[CrossRef](#)]
56. Saruhan, B.; Fomekong, R.L.; Nahiriak, S. High-Sensitivity and -Selectivity Gas Sensors with Nanoparticles, Nanostructures, and Thin Films. *Chemosensors* **2023**, *11*, 81. [[CrossRef](#)]
57. Zhou, Y.; Liu, Y.; Zhang, M.; Feng, Z.; Yu, D.-G.; Wang, K. Electrospun Nanofiber Membranes for Air Filtration: A Review. *Nanomaterials* **2022**, *12*, 1077. [[CrossRef](#)]
58. Thavasi, V.; Singh, G.; Ramakrishna, S. Electrospun Nanofibers in Energy and Environmental Applications. *Energy Environ. Sci.* **2008**, *1*, 205–221. [[CrossRef](#)]
59. Sherlin, V.A.; Baby, J.N.; Sriram, B.; Hsu, Y.-F.; Wang, S.-F.; George, M. Construction of ANbO₃ (A= Na, K)/f-Carbon Nanofiber Composite: Rapid and Real-Time Electrochemical Detection of Hydroxychloroquine in Environmental Samples. *Environ. Res.* **2022**, *215*, 114232. [[CrossRef](#)]
60. Grant, J.J.; Pillai, S.C.; Perova, T.S.; Hehir, S.; Hinder, S.J.; McAfee, M.; Breen, A. Electrospun Fibres of Chitosan/PVP for the Effective Chemotherapeutic Drug Delivery of 5-Fluorouracil. *Chemosensors* **2021**, *9*, 70. [[CrossRef](#)]
61. Song, W.; Tang, Y.; Qian, C.; Kim, B.J.; Liao, Y.; Yu, D.-G. Electrospinning Spinneret: A Bridge between the Visible World and the Invisible Nanostructures. *Innov.* **2023**, *4*, 100381. [[CrossRef](#)]
62. Rahman, N.S.A.; Greish, Y.E.; Mahmoud, S.T.; Qamhieh, N.N.; El-Maghraby, H.F.; Zeze, D. Fabrication and Characterization of Cellulose Acetate-Based Nanofibers and Nanofilms for H₂S Gas Sensing Application. *Carbohydr. Polym.* **2021**, *258*, 117643. [[CrossRef](#)] [[PubMed](#)]
63. Peng, J.; Yuan, H.; Ren, T.; Liu, Z.; Qiao, J.; Ma, Q.; Guo, X.; Ma, G.; Wu, Y. Fluorescent Nanocellulose-Based Hydrogel Incorporating Titanate Nanofibers for Sorption and Detection of Cr(VI). *Int. J. Biol. Macromol.* **2022**, *215*, 625–634. [[CrossRef](#)] [[PubMed](#)]
64. Singh, M.; Pandey, A.; Singh, S.; Singh, S.P. Iron Nanoparticles Decorated Hierarchical Carbon Fiber Forest for the Magnetic Solid-Phase Extraction of Multi-Pesticide Residues from Water Samples. *Chemosphere* **2021**, *282*, 131058. [[CrossRef](#)] [[PubMed](#)]
65. Perez-Rafols, C.; Serrano, N.; Manuel Diaz-Cruz, J.; Arino, C.; Esteban, M. Glutathione Modified Screen-Printed Carbon Nanofiber Electrode for the Voltammetric Determination of Metal Ions in Natural Samples. *Talanta* **2016**, *155*, 8–13. [[CrossRef](#)]
66. Neri, G. Thin 2D: The New Dimensionality in Gas Sensing. *Chemosensors* **2017**, *5*, 21. [[CrossRef](#)]
67. Facure, M.H.M.; Mercante, L.A.; Correa, D.S. Polyacrylonitrile/Reduced Graphene Oxide Free-Standing Nanofibrous Membranes for Detecting Endocrine Disruptors. *ACS Appl. Nano Mater.* **2022**, *5*, 6376–6384. [[CrossRef](#)]
68. Karimi Afshar, S.; Abdorashidi, M.; Dorkoosh, F.A.; Akbari Javar, H. Electrospun Fibers: Versatile Approaches for Controlled Release Applications. *Int. J. Polym. Sci.* **2022**, *2022*, 9116168. [[CrossRef](#)]
69. Zhang, X.; Guo, S.; Qin, Y.; Li, C. Functional Electrospun Nanocomposites for Efficient Oxygen Reduction Reaction. *Chem. Res. Chin. Univ.* **2021**, *37*, 379–393. [[CrossRef](#)]
70. Xu, X.; Lv, H.; Zhang, M.; Wang, M.; Zhou, Y.; Liu, Y.; Yu, D.-G. Recent Progress in Electrospun Nanofibers and Their Applications in Heavy Metal Wastewater Treatment. *Front. Chem. Sci. Eng.* **2023**, *17*, 1–27. [[CrossRef](#)]

71. Huang, C.; Xu, X.; Fu, J.; Yu, D.-G.; Liu, Y. Recent Progress in Electrospun Polyacrylonitrile Nanofiber-Based Wound Dressing. *Polymers* **2022**, *14*, 3266. [[CrossRef](#)]
72. Han, W.; Wang, L.; Li, Q.; Ma, B.; He, C.; Guo, X.; Nie, J.; Ma, G. A Review: Current Status and Emerging Developments on Natural Polymer-Based Electrospun Fibers. *Macromol. Rapid Commun.* **2022**, *43*, 2200456. [[CrossRef](#)]
73. Wang, X.; Feng, C. Chiral Fiber Supramolecular Hydrogels for Tissue Engineering. *Wiley Interdiscip. Rev.-Nanomed. Nanobiotechnol.* **2022**, *14*, e1847. [[CrossRef](#)] [[PubMed](#)]
74. Yu, D.-G.; Du, Y.; Chen, J.; Song, W.; Zhou, T. A Correlation Analysis between Undergraduate Students' Safety Behaviors in the Laboratory and Their Learning Efficiencies. *Behav. Sci.* **2023**, *13*, 127. [[CrossRef](#)] [[PubMed](#)]
75. Wu, Y.; Li, Y.; Lv, G.; Bu, W. Redox Dyshomeostasis Strategy for Tumor Therapy Based on Nanomaterials Chemistry. *Chem. Sci.* **2022**, *13*, 2202–2217. [[CrossRef](#)]
76. Sivan, M.; Madheswaran, D.; Hauzerova, S.; Novotny, V.; Hedvicakova, V.; Jencova, V.; Kostakova, E.K.; Schindler, M.; Lukas, D. AC Electrospinning: Impact of High Voltage and Solvent on the Electrospinnability and Productivity of Polycaprolactone Electrospun Nanofibrous Scaffolds. *Mater. Today Chem.* **2022**, *26*, 101025. [[CrossRef](#)]
77. Sivan, M.; Madheswaran, D.; Valtera, J.; Kostakova, E.K.; Lukas, D. Alternating Current Electrospinning: The Impacts of Various High-Voltage Signal Shapes and Frequencies on the Spinnability and Productivity of Polycaprolactone Nanofibers. *Mater. Des.* **2022**, *213*, 110308. [[CrossRef](#)]
78. Liu, H.; Bai, Y.; Huang, C.; Wang, Y.; Ji, Y.; Du, Y.; Xu, L.; Yu, D.-G.; Bligh, S.W.A. Recent Progress of Electrospun Herbal Medicine Nanofibers. *Biomolecules* **2023**, *13*, 184. [[CrossRef](#)]
79. Shen, Y.; Yu, X.; Cui, J.; Yu, F.; Liu, M.; Chen, Y.; Wu, J.; Sun, B.; Mo, X. Development of Biodegradable Polymeric Stents for the Treatment of Cardiovascular Diseases. *Biomolecules* **2022**, *12*, 1245. [[CrossRef](#)] [[PubMed](#)]
80. Li, C.; Wang, J.; Deng, C.; Wang, R.; Zhang, H. Protocol for Atmospheric Water Harvesting Using in Situ Polymerization Honeycomb Hygroscopic Polymers. *STAR Protoc.* **2022**, *3*, 101780. [[CrossRef](#)]
81. Bai, Y.; Liu, Y.; Lv, H.; Shi, H.; Zhou, W.; Liu, Y.; Yu, D.-G. Processes of Electrospun Polyvinylidene Fluoride-Based Nanofibers, Their Piezoelectric Properties, and Several Fantastic Applications. *Polymers* **2022**, *14*, 4311. [[CrossRef](#)]
82. Kang, S.; Hou, S.; Chen, X.; Yu, D.-G.; Wang, L.; Li, X.; Williams, G.R. Energy-Saving Electrospinning with a Concentric Teflon-Core Rod Spinneret to Create Medicated Nanofibers. *Polymers* **2020**, *12*, 2421. [[CrossRef](#)]
83. Guan, W.; Zhou, W.; Lu, J.; Lu, C. Luminescent Films for Chemo- and Biosensing. *Chem. Soc. Rev.* **2015**, *44*, 6981–7009. [[CrossRef](#)] [[PubMed](#)]
84. Jiang, W.; Zhao, P.; Song, W.; Wang, M.; Yu, D.-G. Electrospun Zein/Polyoxyethylene Core-Sheath Ultrathin Fibers and Their Antibacterial Food Packaging Applications. *Biomolecules* **2022**, *12*, 1110. [[CrossRef](#)] [[PubMed](#)]
85. Yu, D.-G.; Li, Q.; Song, W.; Xu, L.; Zhang, K.; Zhou, T. Advanced Technique-Based Combination of Innovation Education and Safety Education in Higher Education. *J. Chem. Educ.* **2023**, *100*, 507–516. [[CrossRef](#)]
86. Ge, R.; Ji, Y.; Ding, Y.; Huang, C.; He, H.; Yu, D.-G. Electrospun Self-Emulsifying Core-Shell Nanofibers for Effective Delivery of Paclitaxel. *Front. Bioeng. Biotechnol.* **2023**, *11*, 1112338. [[CrossRef](#)] [[PubMed](#)]
87. Huang, X.; Jiang, W.; Zhou, J.; Yu, D.-G.; Liu, H. The Applications of Ferulic-Acid-Loaded Fibrous Films for Fruit Preservation. *Polymers* **2022**, *14*, 4947. [[CrossRef](#)]
88. Li, F.; Song, H.; Yu, W.; Ma, Q.; Dong, X.; Wang, J.; Liu, G. Electrospun TiO₂/SnO₂ Janus Nanofibers and Its Application in Ethanol Sensing. *Mater. Lett.* **2020**, *262*, 127070. [[CrossRef](#)]
89. Jiang, W.; Zhang, X.; Liu, P.; Zhang, Y.; Song, W.; Yu, D.-G.; Lu, X. Electrospun Healthcare Nanofibers from Medicinal Liquor of Phellinus Igniarius. *Adv. Compos. Hybrid Mater.* **2022**, *5*, 3045–3056. [[CrossRef](#)]
90. Zhao, P.; Chen, W.; Feng, Z.; Liu, Y.; Liu, P.; Xie, Y.; Yu, D.-G. Electrospun Nanofibers for Periodontal Treatment: A Recent Progress. *Int. J. Nanomed.* **2022**, *17*, 4137–4162. [[CrossRef](#)] [[PubMed](#)]
91. Lv, H.; Liu, Y.; Zhao, P.; Bai, Y.; Cui, W.; Shen, S.; Liu, Y.; Wang, Z.; Yu, D.G. Insight into the Superior Piezophotocatalytic Performance of BaTiO₃//ZnO Janus Nanofibrous Heterostructures in the Treatment of Multi-Pollutants from water. *Appl. Cata. B Environ.* **2023**, *330*, 122623. [[CrossRef](#)]
92. Wang, P.; Lv, H.; Cao, X.; Liu, Y.; Yu, D.-G. Recent Progress of the Preparation and Application of Electrospun Porous Nanofibers. *Polymers* **2023**, *15*, 921. [[CrossRef](#)] [[PubMed](#)]
93. Ji, X.; Li, R.; Liu, G.; Jia, W.; Sun, M.; Liu, Y.; Luo, Y.; Cheng, Z. Phase Separation-Based Electrospun Janus Nanofibers Loaded with Rana Chensinensis Skin Peptides/Silver Nanoparticles for Wound Healing. *Mater. Des.* **2021**, *207*, 109864. [[CrossRef](#)]
94. Zhou, Y.; Wang, M.; Yan, C.; Liu, H.; Yu, D.-G. Advances in the Application of Electrospun Drug-Loaded Nanofibers in the Treatment of Oral Ulcers. *Biomolecules* **2022**, *12*, 1254. [[CrossRef](#)]
95. Wang, M.; Ge, R.; Zhao, P.; Williams, G.R.; Yu, D.-G.; Annie Bligh, S.W. Exploring wettability difference-driven wetting by utilizing electrospun chimeric Janus microfiber comprising cellulose acetate and polyvinylpyrrolidone. *Mater. Des.* **2023**, *226*, 111652. [[CrossRef](#)]
96. Yu, D.-G.; Zhao, P. The Key Elements for Biomolecules to Biomaterials and to Bioapplications. *Biomolecules* **2022**, *12*, 1234. [[CrossRef](#)]
97. Lv, H.; Guo, S.; Zhang, G.; He, W.; Wu, Y.; Yu, D.-G. Electrospun Structural Hybrids of Acyclovir-Polyacrylonitrile at Acyclovir for Modifying Drug Release. *Polymers* **2021**, *13*, 4286. [[CrossRef](#)] [[PubMed](#)]

98. Knapczyk-Korczak, J.; Zhu, J.; Ura, D.P.; Szewczyk, P.K.; Gruszczynski, A.; Benker, L.; Agarwal, S.; Stachewicz, U. Enhanced Water Harvesting System and Mechanical Performance from Janus Fibers with Polystyrene and Cellulose Acetate. *ACS Sustain. Chem. Eng.* **2021**, *9*, 180–188. [[CrossRef](#)]
99. Wang, M.-L.; Yu, D.-G.; Annie Bligh, S.W. Progress in preparing electrospun Janus fibers and their applications. *Appl. Mater. Today* **2023**, *31*, 101766. [[CrossRef](#)]
100. Li, X.; Niu, X.; Chen, Y.; Yuan, K.; He, W.; Yang, S.; Tang, T.; Yu, D.-G. Electrospinning Micro-Nano Structures on Chitosan Composite Coatings for Enhanced Antibacterial Effect. *Prog. Org. Coat.* **2023**, *174*, 107310. [[CrossRef](#)]
101. Yang, Y.; Chang, S.; Bai, Y.; Du, Y.; Yu, D.-G. Electrospun Triaxial Nanofibers with Middle Blank Cellulose Acetate Layers for Accurate Dual-Stage Drug Release. *Carbohydr. Polym.* **2020**, *243*, 116477. [[CrossRef](#)]
102. Nagiah, N.; Murdock, C.J.; Bhattacharjee, M.; Nair, L.; Laurencin, C.T. Development of Tripolymeric Triaxial Electrospun Fibrous Matrices for Dual Drug Delivery Applications. *Sci. Rep.* **2020**, *10*, 609. [[CrossRef](#)]
103. Wang, M.; Hou, J.; Yu, D.-G.; Li, S.; Zhu, J.; Chen, Z. Electrospun Tri-Layer Nanodepots for Sustained Release of Acyclovir. *J. Alloy. Compd.* **2020**, *846*, 156471. [[CrossRef](#)]
104. Lubasova, D.; Niu, H.; Zhao, X.; Lin, T. Hydrogel Properties of Electrospun Polyvinylpyrrolidone and Polyvinylpyrrolidone/Poly(Acrylic Acid) Blend Nanofibers. *RSC Adv.* **2015**, *5*, 54481–54487. [[CrossRef](#)]
105. Li, C.; Yang, J.; He, W.; Xiong, M.; Niu, X.; Li, X.; Yu, D.-G. A Review on Fabrication and Application of Tunable Hybrid Micro–Nano Array Surfaces. *Adv. Mater. Interfaces.* **2023**, *10*, 2202160. [[CrossRef](#)]
106. Wang, C.; Kaneti, Y.V.; Bando, Y.; Lin, J.; Liu, C.; Li, J.; Yamauchi, Y. Metal–Organic Framework-Derived One-Dimensional Porous or Hollow Carbon-Based Nanofibers for Energy Storage and Conversion. *Mater. Horiz.* **2018**, *5*, 394–407. [[CrossRef](#)]
107. Tang, Y.; Liu, Z.; Zhao, K. Fabrication of Hollow and Porous Polystyrene Fibrous Membranes by Electrospinning Combined with Freeze-Drying for Oil Removal from Water. *J. Appl. Polym. Sci.* **2019**, *136*, 47262. [[CrossRef](#)]
108. Yao, L.; Sun, C.; Lin, H.; Li, G.; Lian, Z.; Song, R.; Zhuang, S.; Zhang, D. Electrospun Bi-Decorated $\text{Bi}_x\text{Ti}_y\text{O}_z/\text{TiO}_2$ Flexible Carbon Nanofibers and Their Applications on Degrading of Organic Pollutants under Solar Radiation. *J. Mater. Sci. Technol.* **2022**, *150*, 114–123. [[CrossRef](#)]
109. Irfan, M.; Uenlue, F.; Le, K.; Fischer, T.; Ullah, H.; Mathur, S. Electrospun Networks of ZnO-SnO₂ Composite Nanowires as Electron Transport Materials for Perovskite Solar Cells. *J. Nanomater.* **2022**, *2022*, 6043406. [[CrossRef](#)]
110. Guo, F.; Guo, Z.; Gao, L.; Qi, D.; Yue, G.; Wang, N.; Zhao, Y.; Li, N.; Xiong, J. Electrospun Core-Shell Hollow Structure Cocatalysts for Enhanced Photocatalytic Activity. *J. Nanomater.* **2021**, *2021*, 9980810. [[CrossRef](#)]
111. Liu, T.; Guo, Y.; Zhang, Z.; Miao, Z.; Zhang, X.; Su, Z. Fabrication of Hollow CuO/PANI Hybrid Nanofibers for Non-Enzymatic Electrochemical Detection of H₂O₂ and Glucose. *Sens. Actuator B-Chem.* **2019**, *286*, 370–376. [[CrossRef](#)]
112. Zhang, J.; Cai, Y.; Hou, X.; Zhou, H.; Qiao, H.; Wei, Q. Preparation of TiO₂ Nanofibrous Membranes with Hierarchical Porosity for Efficient Photocatalytic Degradation. *J. Phys. Chem. C* **2018**, *122*, 8946–8953. [[CrossRef](#)]
113. Yin, D.; Liu, J.; Bo, X.; Guo, L. Cobalt-Iron Selenides Embedded in Porous Carbon Nanofibers for Simultaneous Electrochemical Detection of Trace of Hydroquinone, Catechol and Resorcinol. *Anal. Chim. Acta* **2020**, *1093*, 35–42. [[CrossRef](#)] [[PubMed](#)]
114. Poudel, M.B.; Kim, H.J. Confinement of Zn-Mg-Al-Layered Double Hydroxide and Alpha-Fe₂O₃ Nanorods on Hollow Porous Carbon Nanofibers: A Free-Standing Electrode for Solid-State Symmetric Supercapacitors. *Chem. Eng. J.* **2022**, *429*, 132345. [[CrossRef](#)]
115. Cao, X.; Chen, W.; Zhao, P.; Yang, Y.; Yu, D.-G. Electrospun Porous Nanofibers: Pore-Forming Mechanisms and Applications for Photocatalytic Degradation of Organic Pollutants in Wastewater. *Polymers* **2022**, *14*, 3990. [[CrossRef](#)] [[PubMed](#)]
116. Wang, M.; Meng, G.; Huang, Q.; Qian, Y. Electrospun 1,4-DHAQ-Doped Cellulose Nanofiber Films for Reusable Fluorescence Detection of Trace Cu²⁺ and Further for Cr³⁺. *Environ. Sci. Technol.* **2012**, *46*, 367–373. [[CrossRef](#)] [[PubMed](#)]
117. Atapour, M.; Amoabediny, G.; Ahmadzadeh-Raji, M. Integrated Optical and Electrochemical Detection of Cu²⁺ Ions in Water Using a Sandwich Amino Acidgold Nanoparticle-Based Nano-Biosensor Consisting of a Transparent-Conductive Platform. *RSC Adv.* **2019**, *9*, 8882–8893. [[CrossRef](#)]
118. Bao, J.; Huang, T.; Wang, Z.; Yang, H.; Geng, X.; Xu, G.; Samalo, M.; Sakinati, M.; Huo, D.; Hou, C. 3D Graphene/Copper Oxide Nano-Flowers Based Acetylcholinesterase Biosensor for Sensitive Detection of Organophosphate Pesticides. *Sens. Actuators B Chem.* **2019**, *279*, 95–101. [[CrossRef](#)]
119. Li, M.; Peng, X.; Han, Y.; Fan, L.; Liu, Z.; Guo, Y. Ti₃C₂ MXenes with Intrinsic Peroxidase-Like Activity for Label-Free and Colorimetric Sensing of Proteins. *Microchem. J.* **2021**, *166*, 106238. [[CrossRef](#)]
120. Asghar, N.; Mustafa, G.; Yasinzi, M.; Al-Soud, Y.A.; Lieberzeit, P.A.; Latif, U. Real-Time and Online Monitoring of Glucose Contents by Using Molecular Imprinted Polymer-Based Ides Sensor. *Appl. Biochem. Biotechnol.* **2019**, *189*, 1156–1166. [[CrossRef](#)] [[PubMed](#)]
121. Yao, J.; Ji, P.; Wang, B.; Wang, H.; Chen, S. Color-Tunable Luminescent Macrofibers Based on CdTe QDs-Loaded Bacterial Cellulose Nanofibers for Ph and Glucose Sensing. *Sens. Actuators B-Chem.* **2018**, *254*, 110–119. [[CrossRef](#)]
122. Wang, Y.; Yu, D.-G.; Liu, Y.; Liu, Y.-N. Progress of Electrospun Nanofibrous Carriers for Modifications to Drug Release Profiles. *J. Funct. Biomater.* **2022**, *13*, 289. [[CrossRef](#)]
123. Song, W.; Zhang, M.; Huang, X.; Chen, B.; Ding, Y.; Zhang, Y.; Yu, D.G.; Kim, I. Smart L-Borneol-Loaded Hierarchical Hollow Polymer Nanospheres with Antipollution and Antibacterial Capabilities. *Mater. Today Chem.* **2022**, *26*, 101252. [[CrossRef](#)]

124. Abdel-Karim, R.; Reda, Y.; Abdel-Fattah, A. Review-Nanostructured Materials-Based Nanosensors. *J. Electrochem. Soc.* **2020**, *167*, 037554. [[CrossRef](#)]
125. Afzali, M.; Mostafavi, A.; Nekooie, R.; Jahromi, Z. A Novel Voltammetric Sensor Based on Palladium Nanoparticles/Carbon Nanofibers/Ionic Liquid Modified Carbon Paste Electrode for Sensitive Determination of Anti-Cancer Drug Pemetrexed. *J. Mol. Liq.* **2019**, *282*, 456–465. [[CrossRef](#)]
126. Adhikari, J.; Rizwan, M.; Keasberry, N.A.; Ahmed, M.U. Current Progresses and Trends in Carbon Nanomaterials-Based Electrochemical and Electrochemiluminescence Biosensors. *J. Chin. Chem. Soc.* **2020**, *67*, 937–960. [[CrossRef](#)]
127. Giummarella, N.; Zhang, L.; Henriksson, G.; Lawoko, M. Structural Features of Mildly Fractionated Lignin Carbohydrate Complexes (LCC) from Spruce. *RSC Adv.* **2016**, *6*, 42120–42131. [[CrossRef](#)]
128. Guo, C.; Wang, J.; Chen, X.; Li, Y.; Wu, L.; Zhang, J.; Tao, C. Construction of a Biosensor Based on a Combination of Cytochrome C, Graphene, and Gold Nanoparticles. *Sensors* **2018**, *19*, 40. [[CrossRef](#)] [[PubMed](#)]
129. Chang, M.; Song, T.; Liu, X.; Lin, Q.; He, B.; Ren, J. Cellulose-Based Biosensor for Bio-Molecules Detection in Medical Diagnosis: A Mini-Review. *Curr. Med. Chem.* **2020**, *27*, 4593–4612. [[CrossRef](#)]
130. Kamel, S.; Khattab, T.A. Recent Advances in Cellulose-Based Biosensors for Medical Diagnosis. *Biosensors* **2020**, *10*, 67. [[CrossRef](#)]
131. Ulhakim, M.T.; Rezki, M.; Dewi, K.K.; Abrori, S.A.; Harimurti, S.; Septiani, N.L.W.; Kurnia, K.A.; Setyaningsih, W.; Darmawan, N.; Yulianto, B. Review—Recent Trend on Two-Dimensional Metal-Organic Frameworks for Electrochemical Biosensor Application. *J. Electrochem. Soc.* **2020**, *167*, 136509. [[CrossRef](#)]
132. Zhuo, Y.; Hu, H.; Wang, Y.; Marin, T.; Lu, M. Photonic Crystal Slab Biosensors Fabricated with Helium Ion Lithography (HIL). *Sens. Actuators Phys.* **2019**, *297*, 111493. [[CrossRef](#)]
133. Abraham, P.; Renjini, S.; Vijayan, P.; Nisha, V.; Sreevalsan, K.; Anithakumary, V. Review—Review on the Progress in Electrochemical Detection of Morphine Based on Different Modified Electrodes. *J. Electrochem. Soc.* **2020**, *167*, 037559. [[CrossRef](#)]
134. Wu, D.; Rios-Aguirre, D.; Chounlakone, M.; Camacho-Leon, S.; Voldman, J. Sequentially Multiplexed Amperometry for Electrochemical Biosensors. *Biosens. Bioelectron.* **2018**, *117*, 522–529. [[CrossRef](#)]
135. Daubinger, P.; Kieninger, J.; Unmüßig, T.; Urban, G.A. Electrochemical Characteristics of Nanostructured Platinum Electrodes—A Cyclic Voltammetry Study. *Phys. Chem. Chem. Phys.* **2014**, *16*, 8392–8399. [[CrossRef](#)]
136. Li, D.; Qi, R.; Zhang, L.-Z. Electrochemical Impedance Spectroscopy Analysis of V-I Characteristics and a Fast Prediction Model for PEM-Based Electrolytic Air Dehumidification. *Int. J. Hydrogen Energy* **2019**, *44*, 19533–19546. [[CrossRef](#)]
137. Zhu, Y.; Hang, Y.; Huang, X.; Song, C. Sensitive Determination of Semicarbazide in Flour by Differential Pulse Voltammetry. *J. Anal. Chem.* **2019**, *74*, 913–919. [[CrossRef](#)]
138. Kamel, R.M.; Shahat, A.; Hegazy, W.H.; Khodier, E.M.; Awual, M.R. Efficient Toxic Nitrite Monitoring and Removal from Aqueous Media with Ligand Based Conjugate Materials. *J. Mol. Liq.* **2019**, *285*, 20–26. [[CrossRef](#)]
139. Lucia Campana, A.; Leonardo Florez, S.; Juliana Noguera, M.; Fuentes, O.P.; Ruiz Puentes, P.; Cruz, J.C.; Osmá, J.F. Enzyme-Based Electrochemical Biosensors for Microfluidic Platforms to Detect Pharmaceutical Residues in Wastewater. *Biosensors* **2019**, *9*, 41. [[CrossRef](#)]
140. Vanýsek, P. Two Common Electroanalytical Techniques—Cyclic Voltammetry and Impedance Capacitance Data from Cyclic Voltammetry. *ECS Trans.* **2019**, *41*, 15–24. [[CrossRef](#)]
141. Wen, T.; Yuan, L.; Tian, C.; Jin, Y.; Liu, T.; Yu, J. Preparation and Characterization of (Ca²⁺, Al³⁺)-Infiltrated CaO-Al₂O₃ Auxiliary Electrode for Electrochemical Sulfur Sensor. *J. Ind. Eng. Chem.* **2022**, *106*, 393–399. [[CrossRef](#)]
142. Semenova, E.; Navolotskaya, D.; Ermakov, S. Interrupted Amperometry: The New Possibilities in Electrochemical Measurements. *Pure Appl. Chem.* **2017**, *89*, 1459–1469. [[CrossRef](#)]
143. McCutcheon, K.; Bandara, A.B.; Zuo, Z.; Heflin, J.R.; Inzana, T.J. The Application of a Nanomaterial Optical Fiber Biosensor Assay for Identification of *Brucella* Nomenclatures. *Biosensors* **2019**, *9*, 64. [[CrossRef](#)]
144. McNichols, R.J.; Cote, G.L. Optical Glucose Sensing in Biological Fluids: An Overview. *J. Biomed. Opt.* **2000**, *5*, 5–16. [[CrossRef](#)] [[PubMed](#)]
145. Zhou, L.; Liu, C.; Sun, Z.; Mao, H.; Zhang, L.; Yu, X.; Zhao, J.; Chen, X. Black Phosphorus Based Fiber Optic Biosensor for Ultrasensitive Cancer Diagnosis. *Biosens. Bioelectron.* **2019**, *137*, 140–147. [[CrossRef](#)] [[PubMed](#)]
146. Hou, S.; Feng, T.; Zhao, N.; Zhang, J.; Wang, H.; Liang, N.; Zhao, L. A Carbon Nanoparticle-Peptide Fluorescent Sensor Custom-Made for Simple and Sensitive Detection of Trypsin. *J. Pharm. Anal.* **2020**, *10*, 482–489. [[CrossRef](#)]
147. Li, J.; Liu, X.; Sun, H.; Wang, L.; Zhang, J.; Huang, X.; Deng, L.; Xi, J.; Ma, T. A New Type of Optical Fiber Glucose Biosensor with Enzyme Immobilized by Electrospinning. *IEEE Sens. J.* **2021**, *21*, 16078–16085. [[CrossRef](#)]
148. Naresh, V.; Lee, N. A Review on Biosensors and Recent Development of Nanostructured Materials-Enabled Biosensors. *Sensors* **2021**, *21*, 1109. [[CrossRef](#)]
149. Chen, C.; Wang, J. Optical Biosensors: An Exhaustive and Comprehensive Review. *Analyst* **2020**, *145*, 1605–1628. [[CrossRef](#)]
150. Wu, X.; Yin, J.; Liu, J.; Gu, Y.; Wang, S.; Wang, J. Colorimetric Detection of Glucose Based on the Binding Specificity of a Synthetic Cyclic Peptide. *Analyst* **2020**, *145*, 7234–7241. [[CrossRef](#)]
151. Zheng, S.; Fang, Y.; Chen, Y.; Kong, Q.; Wang, F.; Chen, X. Benzothiazole Derivatives Based Colorimetric and Fluorescent Probes for Detection of Amine/Ammonia and Monitoring the Decomposition of Urea by Urease. *Spectrochim. Acta Part-Mol. Biomol. Spectrosc.* **2022**, *267*, 120616. [[CrossRef](#)]

152. Li, Y.; Wen, Y.; Wang, L.; He, J.; Al-Deyab, S.S.; El-Newehy, M.; Yu, J.; Ding, B. Simultaneous Visual Detection and Removal of Lead(II) Ions with Pyromellitic Dianhydride-Grafted Cellulose Nanofibrous Membranes. *J. Mater. Chem. A* **2015**, *3*, 1818–18189. [[CrossRef](#)]
153. Najarzadegan, H.; Sereshti, H. Development of a Colorimetric Sensor for Nickel Ion Based on Transparent Electrospun Composite Nanofibers of Polycaprolactam-Dimethylglyoxime/Polyvinyl Alcohol. *J. Mater. Sci.* **2016**, *51*, 8645–8654. [[CrossRef](#)]
154. Abou-Omar, M.N.; Attia, M.S.; Afify, H.G.; Amin, M.A.; Boukherroub, R.; Mohamed, E.H. Novel Optical Biosensor Based on a Nano-Gold Coated by Schiff Base Doped in Sol/Gel Matrix for Sensitive Screening of Oncomarker CA-125. *ACS Omega* **2021**, *6*, 20812–20821. [[CrossRef](#)] [[PubMed](#)]
155. Kim, H.-M.; Uh, M.; Jeong, D.H.; Lee, H.-Y.; Park, J.-H.; Lee, S.-K. Localized Surface Plasmon Resonance Biosensor Using Nanopatterned Gold Particles on the Surface of an Optical Fiber. *Sens. Actuators B Chem.* **2019**, *280*, 183–191. [[CrossRef](#)]
156. Marchetti, M.; Ronda, L.; Percudani, R.; Bettati, S. Immobilization of Allantoinase for the Development of an Optical Biosensor of Oxidative Stress States. *Sensors* **2019**, *20*, 196. [[CrossRef](#)]
157. Tang, Y.; Kang, A.; Yang, X.; Hu, L.; Tang, Y.; Li, S.; Xie, Y.; Miao, Q.; Pan, Y.; Zhu, D. A Robust OFF-ON Fluorescent Biosensor for Detection and Clearance of Bacterial Endotoxin by Specific Peptide Based Aggregation Induced Emission. *Sens. Actuators B Chem.* **2020**, *304*, 127300. [[CrossRef](#)]
158. Long, C.; Jiang, Z.; Shangguan, J.; Qing, T.; Zhang, P.; Feng, B. Applications of Carbon Dots in Environmental Pollution Control: A Review. *Chem. Eng. J.* **2021**, *406*, 126848. [[CrossRef](#)]
159. Yuan, H.; Peng, J.; Ren, T.; Luo, Q.; Luo, Y.; Zhang, N.; Huang, Y.; Guo, X.; Wu, Y. Novel Fluorescent Lignin-Based Hydrogel with Cellulose Nanofibers and Carbon Dots for Highly Efficient Adsorption and Detection of Cr(VI). *Sci. Total Environ.* **2021**, *760*, 143395. [[CrossRef](#)]
160. Cai, J.; Ding, L.; Gong, P.; Huang, J. A Colorimetric Detection of MicroRNA-148a in Gastric Cancer by Gold Nanoparticle–RNA Conjugates. *Nanotechnology* **2020**, *31*, 095501. [[CrossRef](#)]
161. Cao, X.; Xia, Z.; Yan, W.; He, S.; Xu, X.; Wei, Z.; Ye, Y.; Zheng, H. Colorimetric Biosensing of Nopaline Synthase Terminator Using Fe₃O₄@Au and Hemin-Functionalized Reduced Graphene Oxide. *Anal. Biochem.* **2020**, *602*, 113798. [[CrossRef](#)] [[PubMed](#)]
162. Fakhri, N.; Abarghoie, S.; Dadmehr, M.; Hosseini, M.; Sabahi, H.; Ganjali, M.R. Paper Based Colorimetric Detection of Mirna-21 Using Ag/Pt Nanoclusters. *Spectrochim. Acta. A. Mol. Biomol. Spectrosc.* **2020**, *227*, 117529. [[CrossRef](#)] [[PubMed](#)]
163. Mulder, D.W.; Phiri, M.M.; Vorster, B.C. Gold Nanostar Colorimetric Detection of Fructosyl Valine as a Potential Future Point of Care Biosensor Candidate for Glycated Haemoglobin Detection. *Biosensors* **2019**, *9*, 100. [[CrossRef](#)] [[PubMed](#)]
164. Shi, H.; Cao, Y.; Xie, Z.; Zhao, Y.; Zhang, C.; Chen, Z. Multi-Parameter Photoelectric Data Fitting for Microfluidic Sweat Colorimetric Analysis. *Sens. Actuators B Chem.* **2022**, *372*, 132644. [[CrossRef](#)]
165. Wei, J.-H.; Yi, J.-W.; Han, M.-L.; Li, B.; Liu, S.; Wu, Y.-P.; Ma, L.-F.; Li, D.-S. A Water-Stable Terbium(III)-Organic Framework as a Chemosensor for Inorganic Ions, Nitro-Containing Compounds and Antibiotics in Aqueous Solutions. *Chem.-Asian J.* **2019**, *14*, 3694–3701. [[CrossRef](#)]
166. Yu, Z.; Huang, W.; Xu, S.; Ke, S. Benzothiazole-Based Colorimetric Chemosensors Bearing Naphthol Aldehyde Unit: Synthesis, Characterization, Selective Detection of Hypochlorite and Its Application as Test Strips. *Microchem. J.* **2021**, *164*, 106009. [[CrossRef](#)]
167. Fan, H.; Zhang, M.; Bhandari, B.; Yang, C. Food Waste as a Carbon Source in Carbon Quantum Dots Technology and Their Applications in Food Safety Detection. *Trends Food Sci. Technol.* **2020**, *95*, 86–96. [[CrossRef](#)]
168. Ye, M.-L.; Zhu, Y.; Lu, Y.; Gan, L.; Zhang, Y.; Zhao, Y.-G. Magnetic Nanomaterials with Unique Nanozymes-like Characteristics for Colorimetric Sensors: A Review. *Talanta* **2021**, *230*, 122299. [[CrossRef](#)]
169. Sahu, S.; Sharma, S.; Kurrey, R.; Ghosh, K.K. Recent Advances on Gold and Silver Nanoparticle-Based Colorimetric Strategies for the Detection of Different Substances and SARS-CoV-2: A Comprehensive Review. *Environ. Sci.-Nano* **2022**, *9*, 3684–3710. [[CrossRef](#)]
170. Hu, L.; Yan, X.-W.; Li, Q.; Zhang, X.-J.; Shan, D. Br-PADAP Embedded in Cellulose Acetate Electrospun Nanofibers: Colorimetric Sensor Strips for Visual Uranyl Recognition. *J. Hazard. Mater.* **2017**, *329*, 205–210. [[CrossRef](#)]
171. Deng, G.; Deng, X.; Deng, J.; Lu, X.; Kang, X.; Song, Y. Performance Evaluation of an Electrospun Nanofiber Mat as Samplers for the Trap of Trace Heavy Metals in Atmospheric Particles and Its Application. *Anal. Sci.* **2020**, *36*, 1453–1459. [[CrossRef](#)]
172. Lee, C.-G.; Na, K.-H.; Kim, W.-T.; Park, D.-C.; Yang, W.-H.; Choi, W.-Y. TiO₂/ZnO Nanofibers Prepared by Electrospinning and Their Photocatalytic Degradation of Methylene Blue Compared with TiO₂ Nanofibers. *Appl. Sci.* **2019**, *9*, 3404. [[CrossRef](#)]
173. Hua, W.; Wang, M.; Li, P.; Shen, K.; Wang, X.; Hsiao, B.S. Sulfonylcalix[4]Arene Functionalized Nanofiber Membranes for Effective Removal and Selective Fluorescence Recognition of Terbium(III) Ions. *New J. Chem.* **2018**, *42*, 6191–6202. [[CrossRef](#)]
174. Chen, R.; Yang, Y.; Wang, N.; Hao, L.; Li, L.; Guo, X.; Zhang, J.; Hu, Y.; Shen, W. Application of Packed Porous Nanofibers-Solid-Phase Extraction for the Detection of Sulfonamide Residues from Environmental Water Samples by Ultra High Performance Liquid Chromatography with Mass Spectrometry. *J. Sep. Sci.* **2015**, *38*, 749–756. [[CrossRef](#)] [[PubMed](#)]
175. Qi, F.; Li, X.; Yang, B.; Rong, F.; Xu, Q. Disks Solid Phase Extraction Based Polypyrrole Functionalized Core-Shell Nanofibers Mat. *Talanta* **2015**, *144*, 129–135. [[CrossRef](#)]
176. Abedalwafa, M.A.; Tang, Z.; Qiao, Y.; Mei, Q.; Yang, G.; Li, Y.; Wang, L. An Aptasensor Strip-Based Colorimetric Determination Method for Kanamycin Using Cellulose Acetate Nanofibers Decorated DNA-Gold Nanoparticle Bioconjugates. *Microchim. Acta* **2020**, *187*, 360. [[CrossRef](#)] [[PubMed](#)]

177. Venkatesan, M.; Veeramuthu, L.; Liang, F.-C.; Chen, W.-C.; Cho, C.-J.; Chen, C.-W.; Chen, J.-Y.; Yan, Y.; Chang, S.-H.; Kuo, C.-C. Evolution of Electrospun Nanofibers Fluorescent and Colorimetric Sensors for Environmental Toxicants, PH, Temperature, and Cancer Cells? A Review with Insights on Applications. *Chem. Eng. J.* **2020**, *397*, 125431. [[CrossRef](#)]
178. Terra, I.A.A.; Sanfelice, R.C.; Valente, G.T.; Correa, D.S. Optical Sensor Based on Fluorescent PMMA/PFO Electrospun Nanofibers for Monitoring Volatile Organic Compounds. *J. Appl. Polym. Sci.* **2018**, *135*, 46128. [[CrossRef](#)]
179. Han, C.; Li, X.; Liu, Y.; Li, X.; Shao, C.; Ri, J.; Ma, J.; Liu, Y. Construction of In₂O₃/ZnO Yolk-Shell Nanofibers for Room-Temperature NO₂ Detection under UV Illumination. *J. Hazard. Mater.* **2021**, *403*, 124093. [[CrossRef](#)]
180. Ngensawat, U.; Pisuchpen, T.; Sritana-anant, Y.; Rodthongkum, N.; Hoven, V.P. Conductive Electrospun Composite Fibers Based on Solid-State Polymerized Poly(3,4-Ethylenedioxythiophene) for Simultaneous Electrochemical Detection of Metal Ions. *Talanta* **2022**, *241*, 123253. [[CrossRef](#)]
181. Deng, Z.X.; Tao, J.W.; Zhao, L.J.; Zhang, W.; Wang, Y.B.; Mu, H.J.; Wu, H.J.; Xu, X.X.; Zheng, W. Effect of Protein Adsorption on Bioelectrochemistry of Electrospun Core-Shell MWCNTs/Gelatin-Hb Nanobelts on Electrode Surface. *Proc. Biochem.* **2020**, *96*, 73–79. [[CrossRef](#)]
182. Jin, X.; Wu, X.; Zhang, F.; Zhao, H.; Zhong, W.; Cao, Y.; Ma, X.; Leng, X.; Zhou, H.; She, M. Cu²⁺ /ATP Reversible Ratiometric Fluorescent Probe through Strip, Hydrogel, and Nanofiber, and Its Application in Living Cells and Edaphic Ecological Safety Assessment. *Dyes. Pigment.* **2020**, *182*, 108677. [[CrossRef](#)]
183. Srinivasan, S.; Nesakumar, N.; Rayappan, J.B.B.; Kulandaiswamy, A.J. Electrochemical Detection of Imidacloprid Using Cu-rGO Composite Nanofibers Modified Glassy Carbon Electrode. *Bull. Environ. Contam. Toxicol.* **2020**, *104*, 449–454. [[CrossRef](#)]
184. Chen, W.; Zhao, P.; Yang, Y.; Yu, D.G. Electrospun beads-on-the-string nanoproducs: Preparation and drug delivery application. *Curr. Drug Deliv.* **2022**, *19*, 1567201819666220525095844.
185. Zhao, P.; Li, H.; Bu, W. A Forward Vision for Chemodynamic Therapy: Issues and Opportunities. *Angew. Chem. Int. Ed.* **2023**, *62*, e202210415. [[CrossRef](#)] [[PubMed](#)]
186. Yao, L.; Sun, C.; Lin, H.; Li, G.; Lian, Z.; Song, R.; Zhuang, S.; Zhang, D. Enhancement of AFB1 Removal Efficiency via Adsorption/Photocatalysis Synergy Using Surface-Modified Electrospun PCL-g-C₃N₄/CQDs Membranes. *Biomolecules* **2023**, *13*, 550. [[CrossRef](#)]
187. Huang, J.; Feng, C. Aniline Dimers Serving as Stable and Efficient Transfer Units for Intermolecular Charge-Carrier Transmission. *Iscience* **2023**, *26*, 105762. [[CrossRef](#)]
188. Wang, Q.; Liu, Q.; Gao, J.; He, J.; Zhang, H.; Ding, J. Stereo Coverage and Overall Stiffness of Biomaterial Arrays Underly Parts of Topography Effects on Cell Adhesion. *ACS Appl. Mater. Interf.* **2023**, *15*, 6142–6155. [[CrossRef](#)]
189. Huang, H.; Song, Y.; Zhang, Y.; Li, Y.; Li, J.; Lu, X.; Wang, C. Electrospun Nanofibers: Current Progress and Applications in Food Systems. *J. Agr. Food Chem.* **2022**, *70*, 1391–1409. [[CrossRef](#)] [[PubMed](#)]
190. Li, H.Y.; Zhang, Z.B.; Ren, Z.T.; Chen, Y.C.; Huang, J.Y.; Lei, Z.X.; Qian, X.M.; Lai, Y.K.; Zhang, S.N. A quadruple biomimetic hydrophilic/hydrophobic Janus composite material integrating Cu(OH)₂ micro-needles and embedded bead-on-string nanofiber membrane for efficient fog harvesting. *Chem. Eng. J.* **2022**, *455*, 140863. [[CrossRef](#)]
191. Xu, J.; Zhong, M.; Song, N.; Wang, C.; Lu, X. General Synthesis of Pt and Ni Co-Doped Porous Carbon Nanofibers to Boost HER Performance in Both Acidic and Alkaline Solutions. *Chin. Chem. Lett.* **2023**, *34*, 107359. [[CrossRef](#)]
192. Zhu, M.M.; Yu, J.Y.; Li, Z.L.; Ding, B. Self-Healing Fibrous Membranes. *Angew. Chem. Int. Ed.* **2022**, *61*, e202208949. [[CrossRef](#)] [[PubMed](#)]
193. Wang, X.; Peng, Y.; Wu, Y.; Cao, S.; Deng, H.; Cao, Z. Chitosan/silk fibroin composite bilayer PCL nanofibrous mats for bone regeneration with enhanced antibacterial properties and improved osteogenic potential. *Int. J. Biolog. Macromol.* **2023**, *230*, 123265. [[CrossRef](#)] [[PubMed](#)]

Disclaimer/Publisher's Note: The statements, opinions and data contained in all publications are solely those of the individual author(s) and contributor(s) and not of MDPI and/or the editor(s). MDPI and/or the editor(s) disclaim responsibility for any injury to people or property resulting from any ideas, methods, instructions or products referred to in the content.